Disposal Strategies Analysis for MEO Orbits

Executive summary

Version 2.0 – 22 December 2015

A.Rossi, E.M.Alessi, G.B. Valsecchi
IFAC-CNR, Italy
H.G. Lewis, C. Colombo
University of Southampton, UK
L. Anselmo. C. Pardini
ISTI-CNR, Italy
F. Deleflie, J. Daquin
IMCCE, Paris, France
M. Vasile, F. Zuiani
University of Starthclyde, UK

ESA Contract No. 4000107201/12/F/MOS

Contractor Study Manager: A. Rossi (IFAC/CNR)
ESA Study Manager: K. Merz (ESA/ESOC)

Table of Contents

1. Introduction

The Medium Earth Orbit (MEO) region, home of the operational Global Navigation Satellite Systems (GNSS) GPS and Glonass, is becoming more and more exploited with the advent of the European Galileo and the Chinese Beidou constellations, both in their build-up phase. The sensitive applications of the navigation satellites and the absence of any natural sink mechanism, such as the atmospheric drag, call for a careful debris prevention policy able to preserve the MEO environment, avoiding in the future the problems now already faced by the LEO and the Geostationary Orbit (GEO) environments.

The analysis of different disposal strategies for the spacecraft belonging to the GNSS, with particular emphasis on the European Galileo system, is the aim of this study.

The possibility to store the disposed spacecraft in stable circular orbits above the operational orbits is the currently adopted strategy and seems, at first sight, the most viable one. Nonetheless, this apparently straightforward procedure is hindered by a few drawbacks. First, the accumulation, in the next decades, of a significant number of spent uncontrolled spacecraft in a limited region of space can give rise to a local collisional activity, with no possibility to control it from the ground with space surveillance means and avoidance manoeuvres. Moreover the noted instability of the GNSS disposal orbits can lead the disposed uncontrolled spacecraft back to dangerous crossings with the operational orbits in a not too distant future ([3][4] [10]).

To tackle these issues, in this study, first, an overview of the current configurations of the GNSSs, along with their operational, maintenance and disposal procedures is given, in Sec. 2. Then, in Sec. 3, an analysis of the dynamics of the orbits in the MEO region is performed. In Sec. 4 the models and software used for the simulations are described and tested. In Sec. 5, with an eye on future applications, alternative methods for de-orbiting of GNSS satellites at end-of-life, exploiting low-thrust propulsion and non-gravitational perturbations, is discussed. Then, in Sec. 6 the results of a large number of numerical simulations of different long term evolution scenarios, implementing different disposal strategies, are shown and discussed. Finally, Sec. 7 presents a detailed analysis of the collision risk and manoeuvres need related to the different scenarios simulated in Sec. 6.

2. Review of MEO GNSS constellation configuration, operation, maintenance and disposal

Since April 1960 (Transit 1B), navigation satellites have been placed in LEO, MEO and GEO, but current operational systems (GPS and GLONASS) are placed in MEO and are complemented by Satellite Based Augmentation Systems (SBAS), generally using spacecraft in GEO, and by Ground Based Augmentation Systems (GBAS). The new generation European navigation system (Galileo) is being deployed in MEO too, and this is also true for the MEO segment of the Chinese Beidou (Compass) system, including also geostationary and inclined geosynchronous orbits.

The basic facts concerning the four navigation satellite constellations in MEO already operational, or in the deployment phase, are summarized in Table 1 [10].

2.1. Constellation maintenance

Currently there are two navigation constellations in MEO fully operational: GPS, since 1994, and GLONASS, since 2011. Galileo and Beidou-M are just in the initial phase of their deployment, to be completed around 2020.

2.1.1. GPS

As of 30 April 2015, 67 GPS spacecraft have been successfully launched. Since 2011, a constellation expansion was carried out, adding eight more slots so that eight extra satellites can be accommodated in the constellation. As a result, GPS can now effectively operate as a 32-slot constellation.

	GPS	GLONASS	GALILEO	BEIDOU-M
Total number of satellites	30	27	30	27
Operational satellites	24	24	24	24
Spare satellites	6	3	6	3
Number of orbit planes	6	3	3	3
Orbital inclination (°)	55 ± 2	65 ± 2	56 ± 2	55 ± 2
Orbital altitude (km)	20,182	19,130	23,222	21,528
Semi-major axis (km)	26,560	25,508	29,600	27,906
Orbital eccentricity	< 0.023	< 0.004	< 0.001	< 0.003
RAAN dispersion (°)	±3	±1	±1	±1
Period of revolution (minutes)	718	676	845	773
Resonance with Earth rotation	(2:1)	(17:8)	(17:10)	(13:7)
Year of first launch	1978	1982	2005	2007

Table 1. Summary of GNSS in MEO

Since 1978, an average of 7 satellites every 4 years has been placed into orbit. In all cases every launch put into orbit a single satellite, because due to the relatively high number of constellation planes (6), such an approach offered the best flexibility in terms of slot filling and gap prevention. This launch strategy will continue to be implemented in the foreseeable future. Concerning the replacement launch rate, an average just a little bit less than 2 launches/satellites per year should be expected also in the coming 2-3 decades.

2.1.2. Glonass

As of 30 April 2015, 128 GLONASS spacecraft have been successfully launched in MEO and 28 are currently active. All the Uragan satellites, and all the Uragan-M until 2010, were launched in triplets using the Proton rocket. In such cases, the upper stages injected the satellites in their final orbit and were left there, in the middle of the constellation. Starting in 2011, the upper stages, after having deployed their satellites in their final orbits, manoeuvred to leave the constellation.
Since 1982, an average of 4 satellites per year was placed into orbit. During the last 15 years, characterised by constellation restoration, the launch rate decreased to 7 satellites every 2 years.
If the “stabilisation” of the operational constellation will be successful, the launch rate is expected to decrease in the future to about 2-3 satellites per year, probably using Soyuz/Fregat-M single shots or equivalent new launchers (e.g. Angara).

2.1.3. Galileo

As of 30 April 2015, disregarding the two Galileo In-Orbit Validation Element (GIOVE) spacecraft, launched in 2005 and 2008 and now decommissioned, a total of 8 operational spacecraft have been deployed, 4 belonging to the In-Orbit Validation (IOV) model, launched in 2011 and 2012, and 4 to the Full Operational Capability (FOC) model. Concerning the latter, Galileo 5 and 6, launched in August 2014, were not able to reach the operational altitude and were finally placed into a lower orbit, attaining a (37:20) resonance with Earth rotation. The launch of Galileo 7 and 8, in March 2015, was instead successful. The design lifetime of the Galileo satellites will not likely exceed 12 years and the constellation will be completed by the end of this decade.
The Fregat-MT stages, with a dry mass of 1030 kg, were disposed a few hundred kilometres above the constellation altitude and outside the GNSS MEO region. Following their decommissioning, the same disposal strategy was adopted for GIOVE-B and, to a lesser extent, for GIOVE-A. However, due to the above mentioned failure, the last but one Fregat-MT stage did not reach the intended

deployment orbit anyway and was abandoned in a 13,712 × 25,878 km of altitude ellipse, inclined by about 50° with respect to the equator. It therefore crossed all the GNSS constellations in MEO.
The deployment of the constellation will be obtained by launching the remaining 18 Galileo-FOC satellites with 3 Soyuz/Fregat-MT (2 satellites per launch) and 3 Ariane-5ES (4 satellites per launch). The launch rate in this phase will be close to 4 satellites per year. After the completion of the constellation, a replacement rate of about 2 satellites (1 double launch) per year is expected.

2.1.4. Beidou-M

As of 30 April 2015, 5 Beidou-M have been successfully launched in MEO: the first (M1), launched with the CZ-3A rocket, carried out on-orbit tests for about 6.4 years, while the following 4, launched in pairs (M3 and M4, M5 and M6) with the CZ-3B rocket, already belonged to the operational model, with a design lifetime of 5 years.
In all these launches, the satellites were deployed into an elliptical Hohmann transfer orbit, so they were placed in the final operational nearly circular orbit in MEO through an apogee manoeuvre carried out with an integrated propulsion system.
Taking into account the requirement to complete the constellation by 2020 and the relatively short design lifetime of the satellites, 2-3 double CZ-3B launches per year should be expected until the end of the decade, during the deployment phase, and a similar launch rate would be needed to maintain the constellation fully operational in the following years. Only when new spacecraft models with a significantly higher design lifetime will become available, the replacement rate will be free to converge towards the GPS value.

2.2. GNSS disposal practices in MEO

The current and foreseen disposal practices for the GNSSs are detailed in the following.

2.2.1. GPS

As of 30 April 2015, taking into account 31 operational satellites and 1 old decommissioned spacecraft maintained as “residual” reserve, the retired GPS satellites in orbit were 35 in total. In addition, 6 Delta-4 and 3 Centaur upper stages used to launch the first 9 Block-IIF spacecraft were present in MEO.
Among the 35 retired GPS satellites, 8 remain close to the operational altitude, possibly including spacecraft which might be reactivated in case of need, while 2 were manoeuvred, respectively, about 90 and 250 km below. All the other 25 satellites were moved, at the end-of-life, in orbits between 220 and 1440 km higher, on average, than the nominal operational altitude of 20,182 km. However, no strategy leading to the control of eccentricity growth was implemented, so the abandoned satellites already cross the GLONASS, GPS and Beidou-M altitudes, with an object density peak just below the Beidou-M operational height. The Galileo altitude will be crossed as well in less than 50 years.
All the 9 upper stages used to deploy the first 9 Block IIF satellites were re-orbited between 450 and 1030 km above the GPS constellation nominal altitude, with initial eccentricity < 0.03, but again no systematic strategy leading to the control of eccentricity growth was implemented, so the Beidou-M constellation is already crossed by 5 stages, while the GLONASS and Galileo operational heights will be reached in several decades by some of them.

2.2.2. GLONASS

The GLONASS satellites resulting abandoned in orbit, as of 30 April 2015, were 100 in total. All were left in the operational orbit. In addition, 92 rocket bodies and released tanks associated with the GLONASS launches were still present in MEO with an apogee higher than 17,000 km,

including 40 Proton upper stages left in the constellation orbits after spacecraft deployment. Therefore, 140 old satellites and upper stages were not disposed outside the constellation.
Notwithstanding the adopted “non-disposal” strategy obviously creates a sharp object density peak at the constellation operational altitude, no other navigation constellation in MEO is crossed by abandoned GLONASS spacecraft and rocket bodies. This situation will not change for at least another 50 years. The crossing of the GPS altitude will need approximately one century to occur, while only after around 150 years the Beidou-M and Galileo altitudes will be affected as well.
The mean altitude of the 7 Fregat-M upper stages was left 290, 330, 370, 391, 339, 320 and 363 km above GLONASS and 762, 722, 682, 661, 714, 733 and 690 km below GPS, with initial eccentricity ≤ 0.01, while that of the Briz-M upper stage of the Proton rocket was lowered by about 950 km below GLONASS, with initial eccentricity $\cong 0.037$. At present it is not clear if the new disposal strategy will become a future standard or not and if it will affect the end-of-life disposal of the satellites as well. Probably the requirement to appropriately dispose the Fregat-MT stages used to deploy the Galileo satellites played a role in devising the new mission profile.
Due to the evolution of the eccentricity, over the next 200 years, the Briz-M upper stage will remain below the GPS constellation, but will cross the GLONASS operational altitude after about 40 years. The three Fregat-M upper stages launched in 2011, on the other hand, will cross the GLONASS height after 30 years and the GPS height in approximately 60 years. Two of them will also reach the Beidou-M altitude in about 110 years and the Galileo altitude in about 140 years. Concerning the four Fregat-M upper stages launched and disposed in 2013 and 2014, Beidou-M and Galileo will remain safe from trajectory interference for more than one century, GPS for approximately 60 years and GLONASS for about 30 years.

2.2.3. Galileo

The Galileo satellites abandoned in orbit, as of 30 April 2015, were the two GIOVE spacecraft. They were originally placed in orbits higher than those of the Galileo system, and at the end-of-life they were left about 118 km (GIOVE-A) and 598 km (GIOVE-B) above the nominal constellation altitude. Galileo 5 and 6 were not able to reach the operational altitude and were finally placed into a lower orbit. Galileo 7 and 8 are not yet positioned in the assigned constellation slot.
For the Galileo satellites and upper stages launched until 2012, a disposal strategy aiming at constraining the long-term eccentricity growth was implemented. This low eccentricity growth condition was guaranteed for at least 200 years in the case of the GIOVE spacecraft and their upper stages, while for the upper stages used to launch the four Galileo-IOV spacecraft the same condition will be met for 100 years.
During the Galileo-FOC deployment phase, in the Soyuz launches, the injection of the 2 satellites occurs in a circular orbit 300 km above the operational constellation and the Fregat-MT upper stage is abandoned there. In the Ariane-5 launches, the injection of the 4 satellites will occur in a circular orbit 300 km below the constellation, and the ES (Evolution Storable) upper stage will be left in such lower orbit. In both cases, it will not be possible to accurately target an optimal argument of perigee, so the goal for the upper stages will be to obtain an orbit as circular and stable as possible, as for the Fregat-MT stage launched in March 2015 [64]. The following injection errors (3σ) can be assumed:

- Soyuz/Fregat-MT upper stage → semi-major axis: 100 km; eccentricity: 0.0018;
- Ariane-5ES upper stage → semi-major axis: 75 km; eccentricity: 0.0012.

2.2.4. Beidou-M

At the beginning of September 2013, the test-bed satellite Beidou-M1 was re-orbited 924 km above the Beidou operational altitude, and 770 km below that of Galileo, in a very low eccentricity (<

10^{-4}) orbit. An inclination reduction, by 3.4°, was carried out as well. The first four operational spacecraft launched in 2012 are instead still functional.

The disposal orbit selected for the first Beidou-M spacecraft was such to limit the long-term eccentricity growth to less than 1.3×10^{-3} for more than 200 years. This will avoid the long-term crossing of any of the four GNSS constellations, limiting the apogee/perigee excursion around the average altitude to < 35 km, a very small value. Even though this single occurrence may not demonstrate that the same, relatively expensive, disposal strategy will be used also in the future, it is anyway indicative of the careful attention paid to the problem of the end-of-life disposal.

All the Beidou-M upper stages have been placed so far in elliptic and short lifetime orbits, avoiding the disposal problem.

2.3. Area and mass of GNSS objects

All the navigation satellites in MEO share the same basic configuration, onsisting of a box-like or cylindrical (in the case of the Uragan and Uragan-M satellites) bus with two wings of solar panels free to rotate around their longitudinal.

According to the NASA Standard 8719.14A (2012), the average random tumbling cross section of a spacecraft can be computed dividing by 4 the total surface area of the satellite bus plus the solar array. So, in order to estimate the average random tumbling cross section of the navigation satellites in MEO, a literature review was carried out in order to collect the relevant information, i.e. bus and solar array sizes and, in addition, the satellite masses. The best data collected or estimated are summarised in Table 2. The best data concerning the upper stages currently used to put into orbit the navigation satellites in MEO, collected [2] or estimated, are summarised in Table 3.

Spacecraft	Bus Size (m)	Solar Array Area (m^2)	Average Random Tumbling Area (m^2)	Mass (kg)	Area to Mass Ratio (m^2/kg)
GPS					
Block I [1,2]		5		455 [3]	
Block II [1,2]		7.3		783 [4]	
Block IIA [1,2]		7.3		870 [4]	
Block IIR [1,2]	1.52 x 1.93 x 1.91	13.4	11.5	980 [4]	0.012
Block IIF [2,5]	1.53 x 1.75 x 2.4	18.4	16.7	1630 [3]	0.010
GLONASS					
Uragan [1,2]	1.2 (∅) x 4.8 (h)	22	16.0	1415 [3]	0.011
Uragan-M [6]	2.4 (∅) x 3.7 (h)	22	20.2	1480 [3]	0.014
Uragan-K1 [7]				935 [3]	
Uragan-K2 [7]					
Uragan-KM [7]				1265 [3]	
GALILEO					
Galileo-IOV [8]	1.58 x 1.59 x 2.74	11	11.1	665 [3]	0.017
Galileo-FOC [2,9]	1.1 x 1.2 x 2.7	11	9.3	665 [3]	0.014
BEIDOU-M					
Beidou-M1 [10]	1.8 x 2.2 x 2.5	22.5	18.2	1000 [11]	0.018
Beidou-M [12] (operational)	2.2 x 2.0 x 3.1	22.5	20.0	800 [13]	0.025

[1] Baker (2002).
[2] Kramer (2002).
[3] On-orbit mass.
[4] Dry mass.
[5] http://nasatech.net/ntGPSIIF-3_PAGE.html.
[6] http://www.navipedia.net/index.php/Main_Page.
[7] http://www.russianspaceweb.com/uragan.html.
[8] Blair (2011); http://www.orbiter-forum.com/showthread.php?t=29226; http://igs.org/mgex/Status_GAL.htm.
[9] Janovsky and Destefanis (2012); Marchlewski (2006); http://en.wikipedia.org/wiki/Galileo_(satellite_navigation).
[10] http://igs.org/mgex/Status_BDS.htm; http://www.dragoninspace.com/navigation/compass-beidou2.aspx.
[11] Estimated taking into account the CZ-3A launcher performances and the propellant mass needed to circularise the final orbit.

Table 2. Navigation satellites in MEO: summary of sizes and masses

Upper Stage	Diameter (m)	Length (m)	Average Random Tumbling Area (m^2)	Mass (kg)	Area to Mass Ratio (m^2/kg)
GPS					
Delta-4-2 R/B	4.0	12.0	33.5	2850	0.012
Atlas-5/Centaur R/B	3.1	12.7	30.4	1914 (14)	0.016
GLONASS					
Fregat-M	3.4	1.5	8.4	920	0.009
Briz-M core stage (15)	2.5	2.6	7.6	1140	0.007
GALILEO					
Fregat-MT	3.4	1.5	8.5	1030	0.008
Ariane-5ES EPS (16)	4.0	3.4	16.4	1275	0.013
BEIDOU-M					
CZ-3B H-18	3.0	12.4	28.0	3062	0.009

Table 3. Upper stages used by navigation satellites in MEO: summary of sizes and masses

3. Definition of initial conditions and dynamical models for further simulations

Orbital resonances are ubiquitous in the Earth orbiting environment, but especially so amongst the highly-inclined, medium-Earth orbits (MEOs) of the Global Navigation Satellite Systems (GNSS), and a clear picture of their physical significance is now of practical interest for the design of disposal strategies for the four constellations. This concerns particularly the question as to whether suitable stable graveyard orbits exist such that satellites in the disposal orbit will not interfere with the GNSSs, or whether strong instabilities exist that can be exploited to permanently clear this region of space from any future collision hazard
We investigated the structure of the web of commensurabilities in the MEO and GTO regions, using a dynamic model accounting for the inhomogeneous, non-spherical gravitational field of the Earth, luni-solar perturbations, and solar radiation pressure. In particular, we studied to what extent the change of initial parameters of storage orbits (the semi-major, eccentricity, and orientation phase angles) can affect the long-term stability of these orbits over centennial and longer timescales. The study is based on the numerical integration of the averaged equations of motion, using a semi-analytic model suitable for all dynamical configurations, which has been approved to be the reference model for the French Space Operations Act (through the software, STELA [1], and its Fortran prototype).
The nominal initial conditions and values of area to mass ratio considered for each constellation in the numerical investigation are displayed in Tabs. 4. The first data set refers to what is called the *graveyard orbit scenario*; the second one to the *eccentricity growth scenario*. These are the same initial conditions used for the simulations described in Sec. 6.
The numerical investigation consisted in propagating these initial conditions for 200 years for a large variety of initial orientation phase parameters and analysing the behaviour of the eccentricity in each case. We considered:

- 36 equally spaced values of ω [0°:360°] in increments of 10°;

[12] http://www.nasaspaceflight.com/2012/09/china-action-dual-compass-launch/.
[13] Estimated taking into account the CZ-3B performances (double launch) and the propellant mass needed to circularise the final orbit.
[14] http://www.braeunig.us/space/specs/atlas.htm.
[15] http://www.russianspaceweb.com/briz.html.
[16] http://www.spacelaunchreport.com/ariane5.html.

- 36 equally spaced values of Ω [0°:360°] in increments of 10°;
- 38 equally spaced initial epochs t_0.

The same analysis has also been performed by increasing and decreasing, respectively, the initial inclination by 1° with respect to the values displayed in Tabs. 4.

			Graveyard orbit scenario				**Eccentricity growth scenario**			
GNSS	A [m^2]	M [kg]	a[km]	Δa[km]	e	i	a[km]	Δa [km]	e	i
Glonass	20.2	1480	26008	500	0.001	65	24293	-1215	0.04895	65
GPS	16.7	1630	27060	500	0.001	55	25271	-1289	0.04996	55
Beidou	20.0	800	28400	494	0.001	55	26520	-1386	0.05122	55
Galileo	9.3	665	30150	550	0.001	56	28086	-1514	0.0539	56

Table 4. Initial mean orbital elements considered for the graveyard orbits and the eccentricity growth scenario of the GNSS constellations, and the corresponding values of area and mass. The variation in semi-major axis Δ*a* with respect to the nominal constellation are also shown

3.1. Simulation results and discussion

We have made our numerical integrations also with the purpose of investigating whether after every Saros a specific configuration of (Ω, ω) leads to the same eccentricity growth. To this end, the majority of the simulations were performed every Δt = Saros/19 ≈ 346.59586 d, starting from t_0 = 26 February 1998 (a solar eclipse epoch) to t_f = 2 Saros. We have chosen this time step because it corresponds to an eclipse year, which is the period of time after which the Moon passes through the same node and the Earth, Moon, and Sun are aligned.
For the graveyard scenario, we noted the following general results:

- No symmetry in the ascending node Ω → Ω + 180° is observed (as expected).
- The symmetry in the argument of perigee ω → ω + 180° cannot be considered as a general rule.
- In general, we always have two narrow lines associated to specific values of initial argument of perigee ω which guarantee stable orbits for any initial epoch and longitude of ascending node (with some exceptions for GLONASS). This bi-modal behaviour can be explained in terms of initial phasing between the satellite and the Moon.
- There also exist large strips, associated with given initial epochs which move according to Ω, that give rise to stable orbits for any value of ω.
- From the above two points, it turns out that the *ω-targeting strategy* is (almost) always feasible for all the constellations for the graveyard scenario with initial nominal inclination. In other words, given any initial epoch and any longitude of ascending node, there exist at least two values of argument of perigee leading to a safe disposal in 200 years.
- The results for Beidou and GPS, in both scenarios, are nearly consistent; somewhat expected given their very close nominal orbits, despite the different area to mass ratios of the constellation satellites (Beidou is almost twice that of GPS). This implies that solar radiation pressure does not have a significant influence on the long-term orbit evolution.
- The semi-major axis does not change significantly in any of the cases explored.
- For the values of inclination explored, the graveyard option is, in general, almost always

possible by targeting a suitable argument of perigee, given (t_0, Ω). Instead, a re-entry within 200 years is far less feasible.

- For the graveyard orbit scenario, the initial inclination ensuring the largest stability opportunities are: 57° for Galileo (i.e., +1°), 66° for Glonass (i.e., +1°), 54° for GPS (i.e., -1°) and 54° for Beidou (i.e., -1°).

  Figures 1 and 2 show the values of ω that can ensure not to cross the operational constellation, given (t_0, Ω), for the three initial values of inclination considered. Note that we have (in general, but not always) at least two values of ω associated with a stable disposal. In these figures, we represent the one corresponding to the minimum eccentricity growth. Moreover, the values of inclination just listed may reflect two kinds of behaviours: either that for the other two values of inclination there exist more (t_0, Ω) initial conditions to which we cannot associate any ω (this is in particular the case of Galileo and GLONASS, see the white dots in the plots), or that for the value of inclination listed for each (t_0, Ω) initial condition we have more ω opportunities than for the other two values of inclination (this is in particular the case of GPS and Beidou, for which we do not have white dots in the plots). The latter behaviour can be ascribed to all the constellations.

  Moreover, note that the worst situation takes place for GLONASS, if the initial inclination is decreased by one degree. For GPS and Beidou, if the initial inclination is increased by 1°, then the number of (t_0, Ω) initial conditions to which we may associate only two values of ω leading to a stable configuration increases noticeable. This reveals the crucial role of the inclination in the stability of the disposal orbits.

- For the eccentricity growth scenario, the initial inclination ensuring largest re-entry opportunities in terms of (t_0, Ω): 56° (the nominal value) for Galileo, 55° ° (the nominal value) for GPS, 56° (i.e., +1°) for Beidou, while re-entry is not possible for Glonass.

  Figure 3 shows the values of ω that can ensure a re-entry into the Earth, given (t_0, Ω) for the three initial values of inclination considered. Also, for GPS we have just slightly more possibilities for i=55° than i=56°. It is however important to remark that in all the cases where a re-entry is computed, it occurs only after at least 100 years for Galileo, 120 years for Beidou and 130 years for GPS.

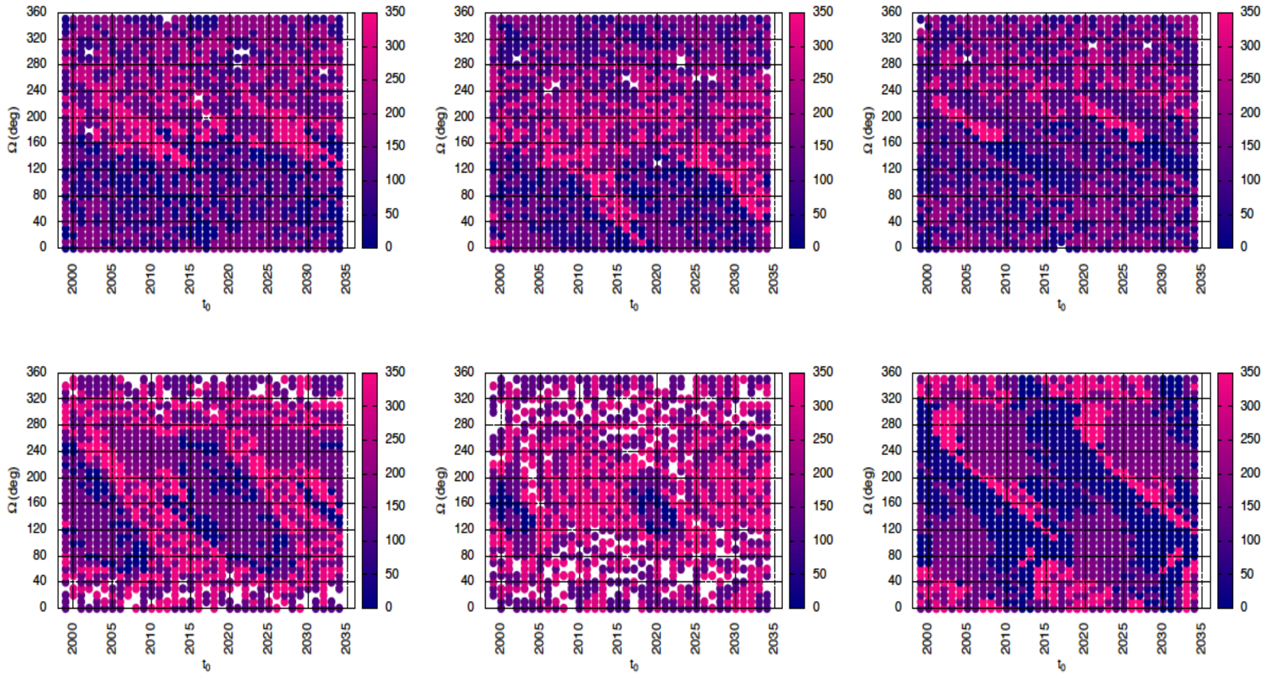

Figure 1. As a function of the initial epoch and longitude of ascending node we show, for the graveyard orbit scenario of Galileo (top) and GLONASS (bottom), the value of argument of pericentre (colour bar) which ensures that the eccentricity will not exceed 0.02 in 200 years. Left: nominal initial inclination; middle: initial inclination decreased by 1 degree; right: initial inclination increased by 1 degree.

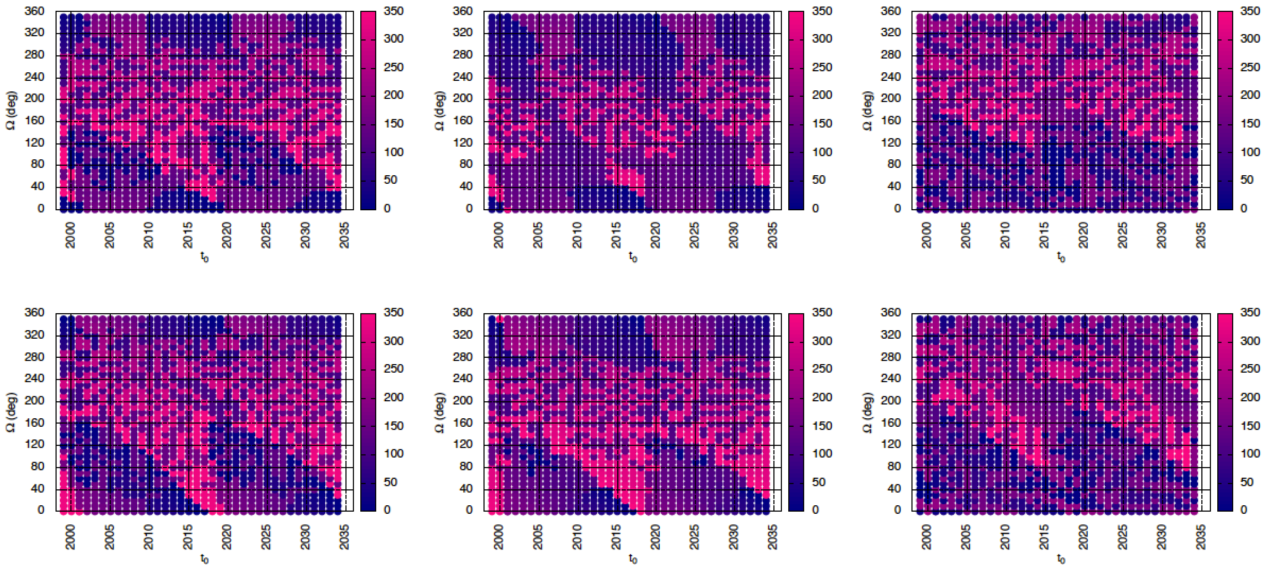

Figure 2. As a function of the initial epoch and longitude of ascending node we show, for the graveyard orbit scenario of GPS (top) and Beidou (bottom), the value of argument of pericentre (colour bar) which ensures that the eccentricity will not exceed 0.02 in 200 years. Left: nominal initial inclination; middle: initial inclination decreased by 1 degree; right: initial inclination increased by 1 degree.

3.1.1. Galileo

For the graveyard orbit scenario, we notice that:

- For any initial value of inclination (nominal, ±1°), the semi-major axis does not change significantly in 200 years (at most 70 km in absolute value) for any (t_0, Ω, ω). Consequently, to avoid interferences with the operational satellites, the eccentricity should not exceed 0.02.

- For any initial value of inclination, the eccentricity can grow up to 0.4 (0.45 only for few cases with an initial inclination decrease). As already noticed, for any given (t_0, Ω) there exist at least two ω initial conditions corresponding to a safe disposal. Moreover, we note (Ω, ω) vertical bands, which move as a function of t_0, and leading to a negligible growth in eccentricity.
- The situation is a little more favourable if the initial inclination is increased by 1°, in the sense that the stable vertical bands are larger.
- Concerning the behaviour in inclination, in the three cases (nominal initial value of inclination, ±1°) its behaviour is organized in Ω bands, which move according to t_0.

For the eccentricity growth scenario, we notice that:

- In the three inclination cases, the eccentricity can increase by up to 0.8 (the minimum eccentricity required to re-enter to the atmosphere is about 0.77). With the nominal initial inclination, the eccentricity growth is remarkable in the entire (t_0, Ω, ω) phase space in the sense that it seems that for any given (t_0, Ω) we may almost always find at least one (but in general more) ω initial condition leading to the re-entry. In the −1° case, re-entry values for *e* can be reached if $\Omega \in$[50°:300°], while in the +1° case the range of Ω depends on t_0. If the satellite node does not match such values, then the eccentricity tends to stay below 0.1.
- Atmospheric re-entries have been computed for the three cases after at least 100 years.
- In the three cases, the inclination can decrease by up to 12° and increase by up to 9°;; it can change by up to +8° and −10°, respectively, in the −1° case; and by up to ±9° in the +1° case. The behaviour is generally structured in islands in the (Ω, ω) space, moving according to t_0.

3.1.2. Glonass

For the graveyard orbit scenario, we notice that:

- For any initial value of inclination (nominal, ±1°), the semi-major axis does not change significantly in 200 years (at most 300 km in absolute value) for any (t_0, Ω, ω). Consequently, to avoid interferences with the operational satellites, the eccentricity should not exceed 0.02.
- Contrary to what happens for the other constellations, we do not always detect two values of ω providing a safe disposal for any (t_0, Ω), but in general only one (except for an inclination increase).
- For the nominal initial inclination, the eccentricity can grow up to 0.5. There exists, however, a large region corresponding to a maximum eccentricity increase up to only 0.05.
- The situation is more favourable if the initial inclination is increased by 1°. The maximum value computed in 200 years for any (t_0, Ω, ω) is 0.25, but only in a few cases. We claim that if the initial node stays in $\Omega \in$[60°:300°], the eccentricity will always not go beyond 0.02.
- Otherwise, if the initial inclination is decreased by 1°, then the eccentricity can grow up to 0.5, and for a given t_0 there exists in general, but not always, only one ω initial condition leading to a safe disposal for any given (t_0, Ω).
- Concerning the behaviour in inclination, in the three cases (nominal initial value of inclination, ±1°) it can increase by at most 3° regularly, in the sense that according to the initial epoch a given Ω band gives rise to the same change in *i* for any ω.

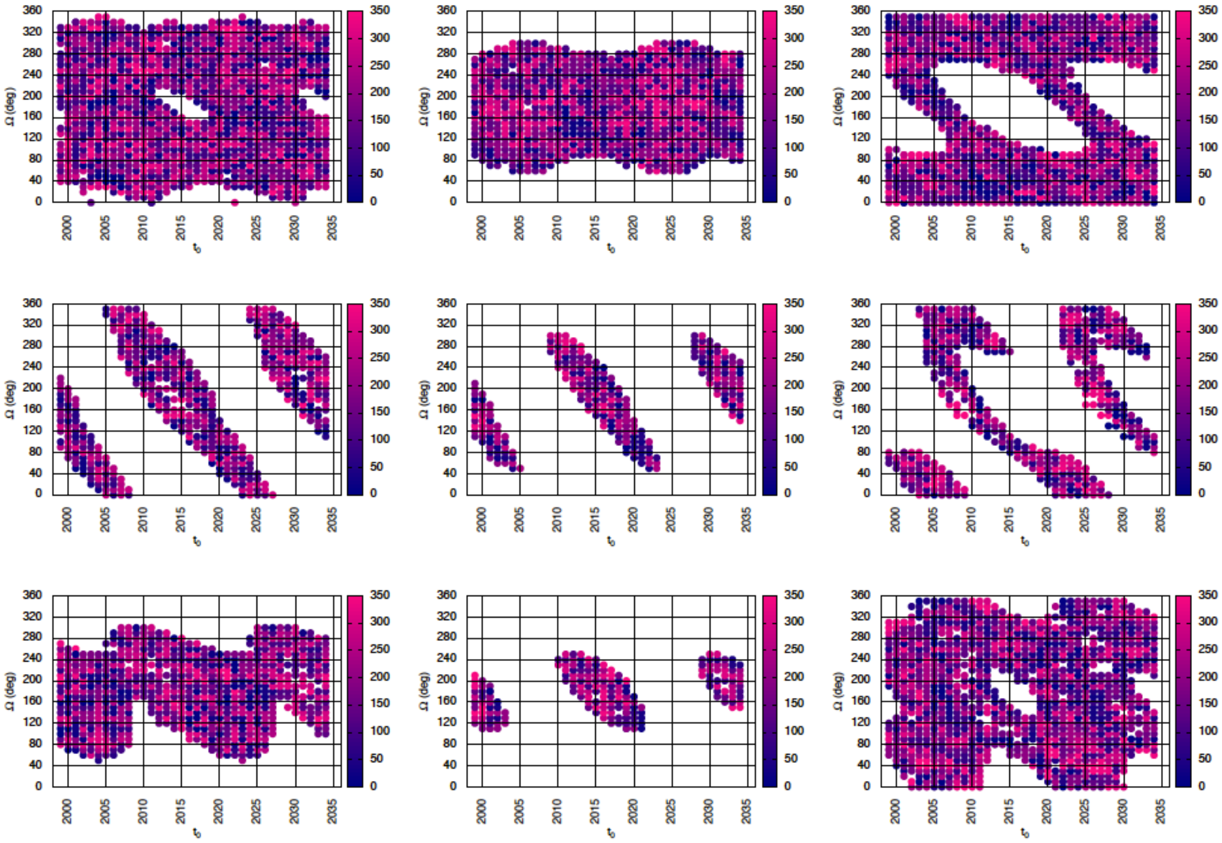

Figure 3. As a function of the initial epoch and longitude of ascending node we show, for the eccentricity growth scenario of Galileo (top), GPS (centre) and Beidou (bottom) (see Table 5), the value of argument of pericentre (colour bar) which ensures a re-entry. Left: nominal initial inclination; middle: initial inclination decreased by 1 degree; right: initial inclination increased by 1 degree.

For the eccentricity growth scenario, we notice that:

- A re-entry is never detected. In the nominal initial inclination and the –1° case, *e* can increase up to 0.7, but not higher (for atmospheric re-entry, the eccentricity must grow to about 0.73).
- As in the graveyard scenario, with an initial inclination of +1° the orbits are relatively more stable: for almost any (t_0, Ω, ω) the maximum valued attained by *e* is about 0.2.
- The inclination can increase by at most 2°. For the most stable initial set (+1° initial inclination), *i* is never lower than 64°. For the other two, a reduction up to 7° can occur.

3.1.3. GPS

For the graveyard orbit scenario, we notice that:

- For any initial value of inclination (nominal, ±1°), the semi-major axis does not change significantly in 200 years (at most 90 km in absolute value) for any (t_0, Ω, ω). This means that to avoid interferences with the operational satellites, the eccentricity should not exceed 0.02.
- For the nominal initial inclination, the eccentricity can grow up to 0.18. The situation is even better if the initial inclination is decreased by 1°.

- If the nominal initial inclination is increased by 1°, then the eccentricity can grow up to 0.2 for any t_0, and it is quite hard to find suitable values of ω ensuring stability for any (t_0, Ω).
- From the above three points, it should be clear that the perigee targeting strategy is feasible, for the nominal initial inclination and if this is decreased by 1°. In the other case, instead, for any given (t_0, Ω) there exist in general only two (few but enough) ω initial conditions corresponding to a safe disposal.
- Each initial set is associated with a maximum increase and decrease in inclination up to 3°.

For the eccentricity growth scenario, we notice that:

- In the three cases, the eccentricity can increase up to 0.8 (the re-entry can occur approximately if $e > 0.74$), but we do not have one ω initial condition leading to the re-entry for any given (t_0, Ω). Atmospheric re-entries have been computed for the three cases after at least 130 years, but not for any t_0.
- In the three cases, the inclination can decrease by up to 8° and increase by up to 7°.

3.1.4. Beidou

For the graveyard orbit scenario, we notice that:

- For any initial value of inclination (nominal, ±1°), in 200 years the semi-major axis does not change significantly (at most 140 km in absolute value) for any (t_0, Ω, ω).This means that to avoid interferences with the operational satellites, the eccentricity should not exceed 0.02.
- For the nominal initial inclination, the eccentricity can grow up to 0.3
- Analogous considerations on the eccentricity can be drawn if the initial inclination is decreased by 1°. In this case, the maximum value computed is 0.25, and the stable configurations correspond to $\Omega \in [50°:300°]$ for any value of (t_0, ω).
- Instead, if the initial inclination is increased by 1°, then the eccentricity can grow up to 0.35, and it is quite hard to find suitable values of ω ensuring stability for any (t_0, Ω).
- From the above three points, it should be clear that the perigee targeting strategy is feasible, for the nominal initial inclination and if this is decreased by 1°. In the other case, instead, for any given (t_0, Ω), there exist in general only two initial ω corresponding to a safe disposal.
- Each initial set is associated with a maximum increase in inclination by up to 4° and decrease by up to 3.5°. We do not detect inclination islands reflecting the eccentricity ones, as noticed for GLONASS, but rather the behaviour is the same as for GPS: the maximum/minimum values correspond to given Ω bands, which move according to t_0.

For the eccentricity growth scenario, we notice that.

- Taking as initial inclination the nominal one or that increased by 1°, the eccentricity can increase up to 0.8 (the re-entry to Earth can happen approximately if $e > 0.75$), but we do not have one ω initial condition leading to the re-entry for any given (t_0, Ω). Depending on the initial epoch, we may have more than one ω initial condition to be targeted, but the strategy is in general not always feasible in terms of always available initial conditions. The same maximum value for e has also been computed for the −1° case, but as long as the t_0 changes, the unstable islands shrink as much as to reduce the maximum value up to only 0.3.
- Consequently, atmospheric re-entries have been computed for the nominal and the +1° initial inclination cases after at least 120 years, for −1° initial inclination configuration after at least 160 years. In the three cases, a successful re-entry depends strongly on the initial

epoch.

- In the three cases, the inclination can decrease, in certain circumstances, to as low as 48°. For the nominal initial inclination case, *i* can grow to 61°, for the −1° case to 58°, and for the +1° case to 64° (i.e., by 8°).

3.2. Conclusions and future recommendations for Galileo

The simulations performed also served as a basis for defining the initial conditions to be used in the environment simulations of Sec. 6. To this end, we extrapolated from the results the values of the argument of perigee ω corresponding to any given combination of initial epoch, longitude of ascending node and inclination (t_0, Ω, *i*), which ensure in 200 years either not to cross the operational satellites for the graveyard orbit scenario or, conversely, the largest possible increase in eccentricity for the eccentricity growth scenario.

The values provided for the simulations of Sec. 6 correspond to Figs. 1 and 3. Note that at the moment there does not exist an analytical formulation to find these initial conditions.

It turns out that we are almost always able to provide initial conditions which can be considered safe over 200 years (except for GLONASS), but we cannot always define initial conditions which lead to an Earth re-entry. This is due to the fact that in practice we do not have the freedom to change (Ω, *i*) to get a more favourable positioning, but more importantly to the intrinsic dynamics where these satellites live. Indeed, the character of the motion depends sensitively upon the initial orientation angles of the satellite and the initial lunar node. This is revealed by the fact that we found large stable regions in the graveyard case for each constellation, even though the constellations exist in such precarious states in the *e*-*i* phase space, always perched on the threshold of instability. The chaoticity of this region also has a further important implication: no matter how accurate our model, once a dynamical instability sets in, the subsequent evolution is unpredictable in detail.

As a matter of fact, the re-entering trajectories computed here exhibit the necessary growth in eccentricity after at least 100 years, which is considered a not reliable time interval because it occurs very likely well beyond the limit time of predictability of the dynamics.

Some other conclusions can be summarized as follows:

- The choice of the initial semi-major axis is not that critical, and this reinforces the statements regarding the importance of tesseral harmonics on the noted instabilities; namely, while such resonances can produce long-term and even chaotic responses in the semi-major axis, since the effects are confined to a very narrow range of semi-major axis (tens of kilometres), they are not of great importance for understanding qualitatively the long-term orbit evolution.

- The influence of the initial inclination is of great importance, in particular when close to the critical inclination, or to the ones inducing a resonant combination. This can be seen, for instance, looking to the graveyard case for GLONASS, GPS and Beidou, for which the acceptable disposal regions reduce considerably if the initial inclination is decreased by 1° and even disappearing completely in the case of GLONASS.

- The dynamics of highly elliptical orbits is much more complex than that of circular orbits. On the one hand, the first order approximation for the third-body perturbation might become too poor to describe the dynamics. On the other hand, as in all cases throughout the Solar System, resonances become wider at larger eccentricity, and therefore different harmonics can interact to produce large-scale instabilities.

4. Review and upgrade of existing models

For this study the SDM and DAMAGE long-term evolution models were used. Both models were adapted and improved to properly simulate the complex management and disposal strategies for the GNSS constellations.
Moreover the orbital propagators used in the models were tested and compared, showing their adequacy for the long-term simulations of the MEO environment.
One of the goals of the study was to identify a disposal strategy for the Galileo constellation that minimizes the collision risk and the manoeuvre frequency for the active satellites.
Both SDM and DAMAGE, in the long term simulations, evaluate the collision risk for a selected spacecraft by using the CUBE algorithm [7]. For the work reported here, the CUBE algorithm can be used as a filter to start a target-centred (and computationally intensive) ellipsoid approach, based on the Foster method [6].

5. MEO de-orbiting with non-gravitational forces

The possibility to de-orbiting from Medium Earth Orbit (MEO) with Low-Thrust (LT) propulsion or the exploitation of solar radiation pressure-augmentation devices was explored, along with the coupling of these two strategies.

5.1. Active de-orbiting from MEO with Low-Thrust propulsion

The preliminary analysis is based on a continuous thrust from a circular orbit in the MEO range to a low Earth orbit with a perigee altitude of 200 km. The simulation model is based on combination of averaging with an analytical solution of low-thrust motion in non-singular orbital elements including the effect of solar pressure, J_2 and the eclipse periods encountered during de-orbiting.
In this study, the motion of the spacecraft is propagated by means of an orbital averaging technique, in which the net variation of the orbital elements along a single revolution is computed; then this averaged over the orbit period and the resulting quantity is integrated numerically over the long time periods. The variation of orbital elements along a single revolution, due to the thrust and other perturbations, is computed by means of an analytical, first-order solution of perturbed Keplerian motion. The contribution of the J_2 perturbation and of the solar radiation pressure is included, as well as thrust and SRP interruptions due to Earth’s shadow.
The de-orbit with LT propulsion of a Galileo-class satellite from MEO was considered. The initial orbit has a semi-major axis a=29600 km, eccentricity e= 0 and inclination, i=55.3 deg.
Initial spacecraft mass, inclusive of the LT propulsion system and its propellant, is assumed to be 1000 kg. The maximum thrust of the propulsion system is not defined a priori, but it is adjusted according to the required de-orbit time. The engine’s specific impulse is assumed to be 3000 s, which is typical of state-of-the-art electric propulsion systems. The thrusting strategy adopted envisions a thrusting arc at apogee with thrust along the negative tangential direction (i.e., decelerating), together with a thrusting arc at perigee with thrust along the positive tangential direction (i.e., accelerating). These have the combined effect of lowering the perigee, while concurrently raising the apogee, thereby increasing the orbit’s ellipticity while retaining a net decrease of the semi-major axis.
If the thrust is applied continuously for the full orbit, the engine thrust requirement is around 0.4 N for the minimum de-orbit time of 0.25 years and is 0.05 N for 2.5 years. Even in the first case, the required thrust is within the capabilities of current electric propulsion systems. Note also that the required thrust decreases exponentially with the de-orbit time. On the other hand, thrusting for the full orbit is somewhat less efficient in terms of propellant consumption, since the required mass, 85 kg, is some 60% higher than the case in which the thrust is applied just for one sixth of each revolution (blue line), i.e., 53 kg. On the other hand, in this latter case, the required thrust, 1.05 N, is

more than double than the “full orbit” case. In this sense, there is a trade-off between required thrust vs. propellant consumption.
For de-orbit times between 2.5 and 25 years the behaviour of the required thrust is very similar to that of the previous case, although the values are obviously one order of magnitude smaller. Note, however, that the propellant mass is basically constant with respect to the de-orbit time.

5.2. De-orbiting from MEO exploiting solar radiation pressure

This section investigates de-orbiting scenarios from Medium Earth Orbit (MEO) exploiting the effect of Solar Radiation Pressure (SRP).
Future missions in MEO region could consider increasing the area to mass of the spacecraft with some inflatable or deployable device in order to artificially increase the effect of solar radiation pressure for a fast increase of the eccentricity. Note that if an inflatable reflective balloon is employed, it does not require any control after deployment and the de-orbit (until re-entry in the atmosphere) can be completely passive [8].
The required effective area to mass-ratio to de-orbit circular orbits changes with inclination and shows high sensitivity with respect to initial orientation. De-orbit with solar radiation pressure only could be achieved with reasonable area to masses for orbits up to 15000 km. In the region from 2000 km altitude to about 7500 km altitude, the required effective area to mass ratio to de-orbit is lower than 10 m^2/kg and can be as low as 1.2 m^2/kg.
GNSS-class spacecraft with altitude around 23,000 km and inclinations between 50 and 70 degrees lie in the range of the figure where the sensitivity to the initial orientation of the de-orbit manoeuvre is high. Thus in this case SRP-augmented de-orbiting would need a fine optimisation of the initialisation manoeuvre. One can conclude that the requirements in effective area to mass ratio for the case of Galileo-class satellite (h = 23,222 km and inclination of 55.3 degrees) are too high for a SRP-only de-orbit.
An alternative solution to decrease the area to mass requirement consists of a strategy to modulate the effect of solar radiation pressure during de-orbiting. Furthermore, the exploitation of solar radiation pressure (and coupling with third body perturbations) and low-thrust propulsion could be considered for GNSS satellites altitudes to decrease the area to mass requirements.

5.2.1. Solar radiation pressure modulation for de-orbiting

An alternative strategy modulates the effect of solar radiation pressure during de-orbiting as a function of the Sun-perigee angle ϕ. The effect of solar radiation pressure is exploited only when the secular and long-term evolution of the eccentricity is positive, while the area to mass increasing device is de-activated, otherwise. In this way, a lower area to mass is required to reach the critical eccentricity, as more than one cycle in the phase space are allowed. The number of cycles is strictly fixed by the maximum time allowed for de-orbiting and determines also the number of time the area to mass increasing device needs to be activated/deactivated. Such an effect can be achieved by changing the attitude of a solar sail with respect to the Sun on an average of 6 months, or by designing a reflective surface with a pyramidal shape, whose area can be controlled. If a simple planar solar sail is chosen, the attitude of the sail must be kept Sun-pointing during the on-arcs, whereas the normal to the sail must be kept perpendicular to the Sun-spacecraft line during the off-arc, so that the effect of SRP is minimised when this would decrease the eccentricity. This effect is also enhanced by the effect of eclipses, as was shown in [5].
SRP-modulation allows decreasing the required area to mass and the requirements for Galileo-like spacecraft are as low as 11.5 m^2/kg; also the dependence on the initial condition in terms of Ω and λ_{Sun} is weaker as more cycles in the phase space are covered.
The cumulative collision probability on re-entry trajectories of the spacecraft with the SRP augmentation device was computed with DAMAGE through 75 Monte Carlo runs for each de-orbit case. The cumulative collision probability for the SRP-dominated de-orbiting cases start equal to

zero and stays small for the initial part of the orbit evolution, increasing only in the last phase of the de-orbiting, when the orbit perigee decreases below 1000 km approximately. Moreover, it should be noted that the SRP-de-orbiting (where the orbit increases in eccentricity) requires a shorter time in the densely populated region than a spiralling down de-orbiting (typical of drag-increasing devices in LEO) and in general a shorter total time for de-orbit.

5.3. Active de-orbiting from MEO with low-thrust propulsion and SRP

A case in which the low-thrust (LT) propulsion and the SRP are concurrently used to de-orbit the spacecraft from MEO was considered too. It is also assumed that the SRP modulation strategy is adopted.

The contribution of the SRP consistently helps in reducing thrust and propellant requirements. Moreover, the impact of the SRP contribution increases with the allowed de-orbiting time. In this sense, while for 2.5 the gains due to SRP are negligible, for 25 years the propellant savings reach around 50% and the thrust is also more than 50% lower.

Looking at the behaviour of the required engine thrust and propellant with respect to the area to mass ratio for a de-orbit in 12 years, it can be noticed how both thrust and propellant decrease linearly with increasing *A/m*.

Due to operational constraints, it may be convenient to limit the low-thrust action to 6 months; afterwards, an area to mass increasing device can be deployed to continue the de-orbiting through SRP-modulation only. The requirements in terms of area to mass and thrust for a de-orbiting from Galileo-like orbit down to 200 km in a range of 5 years and 6 months to 15 years and 6 months was investigated, using two strategies of low-thrust and SRP modulation:

- 6 months of continuous low-thrust along the anti-tangential direction, in order to decrease the energy and spiralling down with a quasi-circular orbit; then SRP modulation;
- 6 months thrusting strategy against the velocity vector across the apogee and along the velocity vector across the perigee to increase the eccentricity; then SRP modulation.

The low-thrust strategy aiming at increasing the eccentricity achieve better. Effective area to mass ratios around 8 m^2/kg are needed for a de-orbiting in 5 years of SRP modulation, after a 6-months active de-orbiting with 0.03 N low-thrust. If the thrust level is increased and the time constraints on the de-orbiting phase with SRP are relaxed, effective area to masses around 1-3 m^2/kg are enough.

5.4. Second generation of Galileo spacecraft: low thrust and SRP de-orbiting

Some preliminary data for second generation of Galileo spacecraft were provided by ESA and are reported in Table 5.

	Small satellite	Large satellite
Thrust [N]	0.18 N	0.265
I_{sp} [s]	3800	1630
Dry mass [kg]	1775	2333
Solar Array surface [m^2]	60	56
Body [m x m x m]	1.1 x 1.1 x 4.5	1.45 x 3.5

Table 5. Preliminary data for second generation Galileo spacecraft.

In order to consider a wider range of possible designs for the next generation of Galileo spacecraft, three thrust levels were considered in this analysis of 0.1 N, 0.2 N and 0.3 N. A low-thrust engine with I_{sp} of 3000 s is used on a 1000 kg spacecraft for deorbiting for a maximum time of 6 months, due to operational ground station constraints; the thrusting strategy is composed of thrusting arcs of 30 degrees around the apogee/perigee. Afterwards, a sail is deployed and SRP modulation is assumed. A reflectivity coefficient of 1.1 is assumed for the satellite and 1.9 for the sail. A very conservative deorbiting requirement is imposed as the altitude at which the deorbiting is considered

successful is 0 km. This is done because drag is neglected in the simulation; it is expected that, in reality drag will enhance the deorbit, therefore the solution proposed here is conservative.
The results depend on the time allowed for deorbiting with the sail (5, 10, 15, 20, 25 y). In the cases on 0.2 and 0.3 N engine, no sail development is needed, since indeed the sail area that would be required is smaller than the solar panels on board the spacecraft. Only in case of a 0.1 N (which is anyway below the one considered for the small satellite design in Table 5) a second phase with SRP modulation would be required and the sail requirements are represented in the first and fourth columns of Table 6.

Deorbiting time [years]	**Sail area [m^2]**			**Sail size [m]**		
	Thrust [N]			**Thrust [N]**		
	0.1 Small satellite	**0.2 Small satellite**	**0.3 Large satellite**	**0.1 Small satellite**	**0.2 Small satellite**	**0.3 Large satellite**
5	4484.21	n/a	n/a	66.96	n/a	n/a
10	2428.95	n/a	n/a	49.28	n/a	n/a
15	1868.42	n/a	n/a	43.23	n/a	n/a
20	1121.05	n/a	n/a	33.48	n/a	n/a
25	962.24	n/a	n/a	31.02	n/a	n/a

Table 6. Sail requirements for second generation Galileo spacecraft considering spacecraft parameters in Table 5 (for the three value of thrust considered the closest design of spacecraft parameter in Table 3 is associated).

It was found that:

- A 6 months deorbiting is achievable with a low-thrust engine with T=0.2 or 0.3 N
- The best low-thrust strategy is the one that aims at increasing the eccentricity, however a different re-entry angle is achieved than re-entering with a spiralling trajectory.
- If the low-thrust engine has a limit of 0.1 N thrust for 6 month operational time, a deployable device can be also used afterwards with SRP modulation for completing the deorbiting phase.
- The collision expectancy cumulated along the whole disposal trajectory was computed. It remains globally low (a few times 10^{-3}) and clearly shows a step increase starting at the epoch of the first interactions with the crowded LEO region.

5.5. MEO de-orbiting with low-thrust and non-gravitational perturbations: conclusions

In conclusion, opportunities for deorbiting circular MEO spacecraft comprehends:

- SRP augmented deorbiting (passive). This passive deorbiting strategy has been shown to be feasible for small spacecraft. Due to the exploitation of SRP and drag, is characterised by uncertainty in the re-entry point. For this reason it can be applied to low-mass and low-re-entry survival chances. It should also be considered that an increased area-to-mass-ratio increases the risk of collisions during the deorbiting (higher for drag augmentation), however it shorten the deorbit time and in some cases it makes re-entry achievable.
- SRP augmented deorbiting (active). SRP modulation allows decreasing the area-to-mass requirements but need a system solution for multiple deployments. SRP modulation would require folding/deploying a reflective area with every 6 months
- Low-thrust can provide deorbiting with reasonable thrust level and mass consumption if the de-orbit time is long enough.
- Low-thrust + SRP combination allows savings in engine size and propellant (up to 40-50%).

6. Long term simulations setup and analysis

Following the theoretical analysis performed in the previous Work Packages, a massive simulation task was performed to study the effect of different management strategies of GNSSs on the long term evolution of the MEO environment.
A detailed simulations setup was defined for the various scenarios envisaged in the study.
Beyond the GNSS management procedures detailed here, all the scenarios share the same main assumptions and a common simulation plan for the LEO and GEO traffic. In particular:

- the initial population consists of the objects *larger than 5 cm*, taken from MASTER;
- the simulations consider the whole circum-terrestrial space, from LEO to GEO;
- the launch traffic cyclically mimics the activity of the past decade;
- an 8-year mission lifetime for future spacecraft is assumed;
- the post-mission disposals measures are applied to upper stages and spacecraft with *60 % success rate*;
- the future explosions are set to zero;
- no station-keeping and no collision avoidance manoeuvre are allowed;
- the NASA Breakup model is used;
- 200 years projections are performed.
- 50 Monte Carlo runs are performed for each scenario.

6.1.1. Reference scenario

The Reference Scenario is the main scenario against which all the others will be compared. It is basically a revised “business-as-usual” scenario where most of the maintenance practices currently adopted by the different constellations are simulated. In some cases, the simulated procedures might not be exactly the same adopted by a particular constellations in the recent past, but instead what are deemed to be the most probable procedures for the near future operations of that system.
In every constellation we assume that the success rate of the end-of-life disposal will be 90% (at difference to what is simulated for the LEO spacecraft, for which a success rate of 60 % is assumed).
Note that, irrespective of the simulated scenario, unless explicitly mentioned, the spacecraft are always disposed to orbits having the same inclination of the operational orbit *at the epoch of disposal* (i.e., the inclination is routinely propagated during the simulation time span and no inclination change manoeuvre is done at the disposal epoch). Similarly, the right ascension of the node (RAAN) of each object is evolved in time and, at end-of-life, the disposal is done on the same orbital plane of the operational satellite *at the epoch of disposal* (i.e., no change of RAAN in performed with the disposal manoeuvre).
The details of the configuration, launch, maintenance and disposal strategies adopted for the four GNSSs simulated are given in Table 7 and Table 8. Note that, when an interval is indicated, the actual value is randomly drawn from a flat rectangular distribution within the interval. For all the constellations the success rate of the end-of-life disposal will be 90%.

	GPS	**Glonass**	**Galileo**	**Beidou**
a [km]	26560	25508	29600	27906
e	<0.023	<0.004	<0.001	<0.001
e [deg]	55° ± 2°	65° ± 2°	56° ± 2°.	55° ± 2°
Orbit planes	6	3	3	3

Total number of satellites (including spares)	30	27	30	27
Total number of satellites per plane	5	9	10	9
Satellite average lifetime [years]	10	8	10	10
Satellite mass [kg]	1630	1480	665	800
Satellite random tumbling average area [m^2]	16.7	20.2	9.3	20
Upper stage mass [kg]	2850	920	1480	3062
Upper stage random tumbling average area [m^2]	33.5	8.4	8.5	28

Table 7. Configuration of the four simulated GNSSs.

6.1.2. *Stable and unstable scenarios*

Before detailing the other simulation scenarios, an introduction to the computational method used in SDM_MEO 1.0 for the end-of-life disposal on stable or unstable orbits is given.

6.1.2.1 The matrix method

Based on the results of MEO dynamics analysis, the spacecraft of all four GNSS constellations in MEO will be disposed at the end-of-life in orbits where either the minimal or maximal eccentricity growth is foreseen.
When a spacecraft reaches the end-of-life some of its orbital elements can be changed with a series of impulsive maneuvers, taking into account the available propellant. Disregarding the mean anomaly, these elements are the semimajor axis (a) the eccentricity (e) and the argument of perigee (ω). In some cases it would be beneficial to change also the inclination and the Right Ascension of the Ascending Node (RAAN), but it is well known that the change in the orbital plane implied by a change of these elements would require a very expensive maneuver, almost always incompatible with the available Delta V. Therefore, the inclination and the RAAN of the disposal orbit are kept equal to the ones of the specific satellite operational orbit at the epoch of disposal.
As detailed in the Sec. 3, an analytical expression able to catch the whole complexity of the long term behaviour of the eccentricity in the MEO orbital region over the 200-year time span is not currently available.
In the end, what is needed for the purpose of identifying the best disposal orbit is an algorithm that allows to choose the proper values of a, e and ω, given i and RAAN at the disposal epoch, that guarantee the desired long term behaviour of the eccentricity. From the practical point of view of the SDM long term simulations, the values of the disposal semimajor axis and eccentricity are dictated by the available Delta V, and can therefore be considered fixed (i.e., given in input).
Therefore we are left with the choice of the argument of perigee given a set of 4 orbital elements.
In Sec. 3, given the nominal disposal semimajor axis and eccentricity, a large number of numerical integrations were performed, sampling the ω-*RAAN* space (from 0 to 360 degrees, at steps of 10 degrees). For all the cases the time history of all the orbital elements is available. Looking at the growth of the eccentricity, maps of the phase space like those shown in Figs. 1-3 were produced, for every GNSSs, both for the case of circular disposal orbits and for the case of eccentric disposal orbits (in this case, the disposed satellite is assigned an initial eccentricity equal to the value used for the computation of the matrix, i.e., e_{disp}=0.0539±0.001).

	GPS	**Glonass**	**Galileo**	**Beidou**
Launches (build-up)	N/A	N/A	2 double launches per year with Soyuz-STB/ Fregat-MT	3 double launches per year with CZ-3B
Launches (constellation	1-2 single launches per year with Delta-4	2-3 single launches per year with Soyuz-	1 double launch per year with Soyuz-STB/Fregat-MT	2 double launches per year with

maintenance)		2-b/Fregat-M		CZ-3B
Spacecraft orbit keeping	No control of RAAN and inclination is foreseen	No control of RAAN and inclination is foreseen	The RAAN of the planes will be kept within a 2° window, i.e. ± 1° around the nominal precessing value. The satellites are launched at one extreme of the control window, so that the slow precession of the nodes will remain within the desired boundaries without the need of a control manoeuvre during the spacecraft lifetime. In in the simulations the satellites will be placed not in the centre of the window, but at the "right" extreme value.	No control of RAAN and inclination is foreseen.
Spacecraft disposal	Re-orbiting 500 ± 10 km above the operational altitude. No targeting of a stable resonant angle will be carried out. Initial ecc. < 0.01.	Re-orbiting 500 ± 10 km above the operational altitude. No targeting of a stable resonant angle will be carried out. Initial ecc. < 0.01.	For the Galileo satellites at the end-of-life, a re-orbiting ΔV budget of approximately 100 ± 10 m/s will be considered, which is translated into a re-orbiting altitude of about 800 km above the constellation altitude. An upper limit of about 800 km above the operational altitude will be considered for the circular disposal orbits, even if the available ΔV would allow a higher disposal. The value applied to each satellite will be extracted between 750 and 800 km. No targeting of a stable resonant angle will be carried out. Initial ecc. < 0.001.	Re-orbiting 500 ± 10 km above the operational altitude. No targeting of a stable resonant angle will be carried out. Initial ecc.< 0.01.
Upper stages disposal	Delta-4 second stages left 950 ± 100 km above the constellation altitude, with eccentricity ≤ 0.01. No targeting of a stable resonant angle will be carried out.	Fregat-M stages left 300 ± 100 km above the constellation altitude, with eccentricity ≤ 0.01. No targeting of a stable resonant angle will be carried out.	Upper stages (Fregat-MT) left 310 ± 10 km above the constellation altitude, with eccentricity ≤ 0.0006.	CZ-3B third stages left in 150 × 21,500 km elliptical transfer orbit.

Table 8. Details of the launch, maintenance and disposal strategies for the simulated GNSSs.

In the *matrix method*, implemented in SDM_MEO 1.0, these plots are translated in matricial form and stored in ASCII files, for each navigation constellation. Every time a spacecraft, belonging to a

GNSS, has to be de-orbited, according to the scenario simulated (e.g., stable or unstable), the deorbiting algorithm searches within the matrices, for the given epoch and for the RAAN of the epoch, the (single) value of ω that minimizes or maximizes the eccentricity growth.
Note that the matrices were computed considering the nominal GNSSs inclinations. During the SDM runs, as a default, the slight difference between the inclination of the satellites to be disposed and the nominal inclination for whom the matrix was computed is neglected. A further set of simulations, with matrices computed for different inclinations close to the nominal one, were performed.

6.1.2.2 *Stable scenario: minimal eccentricity growth*

The spacecraft of all four GNSS constellations in MEO will be disposed at the end-of-life in orbits where the minimal eccentricity growth is expected, taking into account the proper angular arguments obtained with the matrix method. That is, the elements of the disposal orbits are the same as those used in the Reference case, except for the argument of perigee which is selected with the matrix method.

6.1.2.3 *Unstable scenario: maximal eccentricity growth*

In this case the spacecraft will be put in disposal orbits as unstable as possible, again by properly targeting the argument of perigee using the matrix method. In particular:

- an initial disposal manoeuvre with a $\Delta V \sim 100$ m/sec is performed to increase the eccentricity. The value of the initial disposal eccentricity reached for all the four navigation constellations is about 0.05 ± 0.001. The disposal semimajor axis is such that the initial apogee of the disposal orbit is at the altitude of the operational orbit, plus (or minus) the spread.
- the optimal value of the argument of perigee, ω, leading to a fast eccentricity growth is selected from the proper matrix.

6.1.2.4 *Stable and Unstable Galileo scenarios*

The simulation scenario is similar to the Stable scenario. The difference here is that, in this case, only the Galileo spacecraft will be disposed with a targeting of the optimal argument of perigee. The satellites of the other constellations will be disposed as in the Reference Case. The purpose of these simulations is to highlight the potential benefits, if any, of a “proper” disposal management of the Galileo constellation alone.

6.1.2.5 *Stable and Unstable scenarios with inclination change*

The actual inclination of the constellation orbits can vary with respect to the nominal values by about ± 1 degree, due to launch dispersions and orbital perturbations. As detailed in Sec. 3, the stability/instability zones in the phase space are sensitive to small inclination changes. Since orbital maneuvers to change the inclination are very expensive in terms of ΔV, it is not very realistic to simulate orbital plane changes to target the preferred regions of phase space. Therefore, there is the risk to miss the right argument of perigee with the matrix method.
For this reason it was decided to repeat the stable and unstable simulation scenarios, described above, taking into account the actual orbital inclination at the epoch of the disposal. For this purpose, different matrices were computed for disposal orbits having inclination ± 1 degree around the nominal orbits. At the moment of the disposal maneuver, the algorithm is using the matrix that refers to the inclination closer to the actual orbital inclination of the epoch.

6.2. Simulation results

Although all the simulations were performed considering the whole circumterrestrial space, the focus of the following analysis will be on the MEO region and, in particular, on the GNSSs related spacecraft. The LEO environment is not the goal of this study. Nonetheless, it is worth stressing that the LEO population evolution is fully evolved and is duly considered to properly account for the collision risk of MEO spacecraft on eccentric orbits that might be crossing LEO at perigee. As written in Sec. 6 all the simulations consider objects larger than 5 cm.

6.2.1. Main scenarios results

Figure 4 (left panel) shows the time evolution of the effective number of objects, larger than 5 cm, in the region between 15000 and 35000 km. The thick lines are the average over 50 MC runs in the three scenarios (as detailed in the figure caption), while the thin red lines are the ± 1 sigma uncertainty interval, coming from the MC averaging process of the Reference case (the 1 sigma lines for the other two cases are not shown to avoid cluttering). It is immediately clear that, looking in terms of the number of objects, the three scenarios are basically statistically indistinguishable. At variance from the LEO region, the environment evolution in MEO is driven mostly by the deterministic pace of the launch and removal actions and by a very limited number of collisional fragmentations. It is worth stressing that the large width of the 1 sigma bars in Figure 4 (left panel) is due to the fact that the pace of the growth is due to a very small number of collisions changing significantly the number of objects from one MC occurrence from the others.

The right panel of Figure 4 shows the time evolution of the number of objects larger than 5 cm, divided by object types. Note the linear pace of the intact spacecraft in contrast with the more than linear pace of the fragments.

Table 9 lists all the collisional fragmentations recorded in all the MC runs, involving a spacecraft belonging to one of the GNSSs in the three scenarios.

It can be noticed how, on average, we can expect less than one collision in the 200-year time span. It is worth noting that only the first entry in the table involved an operational spacecraft, so that one might assume that "in reality" this collision could have been avoided with a proper maneuver triggered by the space surveillance systems. On the other hand, all the other fragmentations involve only disposed, non maneuverable, spacecraft. It can also be noticed that the majority of the collisions are recorded in the Stable cases. Despite the small number of events, this might be a first indication that the accumulation of uncontrolled spacecraft in the disposal regions above the operational orbits can be the source of a future

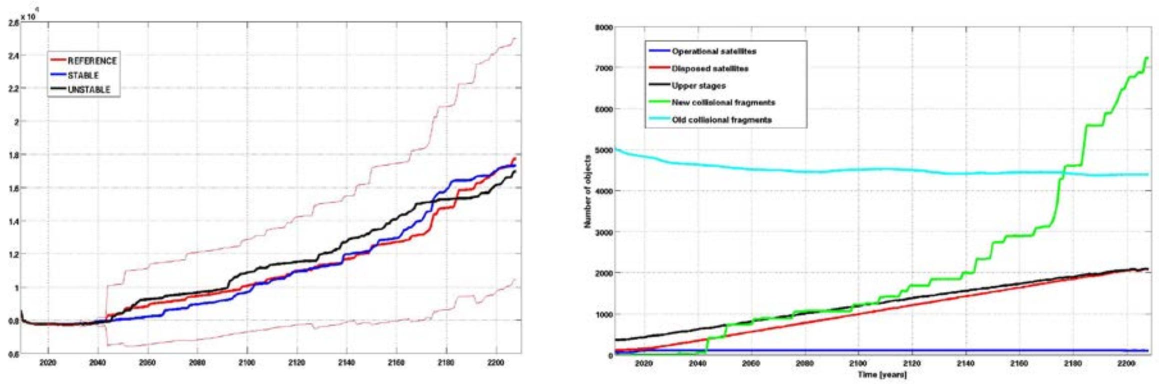

collision activity.

Figure 4. Left panel: Effective number of objects between 15000 and 35000 km, larger than 5 cm in the three scenarios: Reference (thick red line), Stable (blue line) and Unstable (black line). The thin red lines show the ± 1 sigma of the MC averaging in the Reference case. Right panel: Effective number of objects between 15000 and 35000 km, larger than 5 cm divided by type: operational satellites (blue), disposed satellites (red), upper stages (black), old collisional fragments (cyan) and new collisional fragments (green).

Scenario	Year of event	T. a [km]	T. e	T. i [deg]	T. Type	P. a [km]	P. e	P. i[deg]	P. Type
Reference	2075	26560	0.0051	55.48	Operational GPS	26577	0.0061	64.75	Disposed Glonass
Reference	2173	27358	0.0028	53.88	Disposed Beidou	27411	0.0010	57.72	Disposed Beidou
Stable	2109	25932	0.0004	66.15	Disposed Glonass	25810	0.0051	63.05	Upper stage
Stable	2167	27060	0.0004	53.08	Disposed GPS	27060	0.0008	56.74	Disposed GPS
Stable	2171	25988	0.0026	65.02	Disposed Glonass	25990	0.0014	63.69	Disposed Glonass
Stable	2179	26036	0.0027	65.75	Disposed Glonass	25810	0.0131	64.27	Upper stage
Stable	2181	28374	0.0007	52.86	Disposed Beidou	28403	0.0005	52.12	Disposed Beidou
Unstable	2056	26580	0.0951	55.96	Disposed Beidou	26567	0.0512	54.80	Disposed Beidou
Unstable	2206	24258	0.0764	65.80	Disposed Glonass	24322	0.0511	62.95	Disposed Glonass

Table 9. List of all the collisional fragmentations recorded in the whole set of MC runs performed in the three scenarios, involving, at least, one object belonging to one of GNSSs. The columns list: the year of the event, the semimajor axis, eccentricity, inclination and object type of the target (T) and of the projectile (P).

Note that, no feedback collisions, i.e., no collisions between fragments generated in the events of Table 9 and other GNSS related objects, are recorded in any MC run.
As indicated in Table 9, all the collisions involving GNSSs objects happen on circular orbits in the MEO region. A few collisional fragmentations are happening also in highly elliptical orbits, mostly of Molniya type, during their LEO crossings at perigee.

6.2.1.1 *Eccentricity evolution*

Due to the assumptions in the three main scenarios, detailed in Sec. 6, we expect a different long term evolution of the orbits of the disposed objects, i.e., mainly in the growth of the eccentricities. Some statistical measures of the eccentricity distribution, at the end of the 200-year time span, for all the disposed GNSS satellites, in the three scenarios are listed in Table 10. Table 11 shows the values of the different statistical measures for each constellation.

	Mean	Standard Deviation	50^{th} percentile (median)	75^{th} percentile	90^{th} percentile
Reference	0.0404	0.0735	0.0122	0.0394	0.1119
Stable	0.0110	0.0272	0.0024	0.0086	0.0258
Unstable	0.1338	0.1455	0.0752	0.1839	0.3540

Table 10. Statistical measures of the eccentricity distribution, in the year 2209, for the three main simulation scenarios.

	Mean	Standard deviation	50th percentile (median)	75th percentile	90th percentile
Glonass (Reference)	0.0484	0.0879	0.0126	0.0449	0.1410
Glonass (Stable)	0.0098	0.0247	0.0018	0.0067	0.0250
Glonass (Unstable)	0.1414	0.1328	0.0816	0.2381	0.3543
GPS (Reference)	0.0523	0.0851	0.0159	0.0570	0.1578
GPS (Stable)	0.0089	0.0279	0.0020	0.0063	0.0175
GPS (Unstable)	0.1345	0.1305	0.0859	0.1715	0.3169
Beidou (Reference)	0.0294	0.0522	0.0108	0.0299	0.0756
Beidou (Stable)	0.0069	0.0155	0.0019	0.0056	0.0166
Beidou (Unstable)	0.1355	0.1516	0.0746	0.1730	0.3548
Galileo (Reference)	0.0487	0.0751	0.0206	0.0542	0.1281
Galileo (Stable)	0.0257	0.0425	0.0110	0.0249	0.0667
Galileo (Unstable)	0.1595	0.1682	0.0875	0.2252	0.4230

Table 11: Statistical measures of the eccentricities of the disposed spacecraft in the years 2209, for each constellation in the three scenarios.

The global eccentricity values show how the proper choice of the initial disposal angles, performed with the matrix method, allows a better stability or instability of the disposal orbits.
Considering the eccentricities that the uncontrolled disposed satellites must keep in order not to interfere with the operational GNSSs it can be noticed how, while in the Reference case the mean eccentricity for all the constellations is above the allowed eccentricity values, in the Stable case the limiting values are not exceeded, with the exception of the Galileo disposed spacecraft for which the mean value of the eccentricity is exceeding the maximum allowed value (whereas the median is below the maximum allowed value).This is related to the noted larger instability of the Galileo orbits and to the presence, in the examined sample, of about 10 % of satellite for whom the disposal manoeuvre did not succeed and that are therefore allowed to reach higher values of the eccentricity.
In any case it can be stated that, on average, the disposed spacecraft are not interfering with the operational ones, both within one GNSS and with the neighbouring ones.
On the other hand, the eccentricity reached in the unstable case while clearly larger than in the other two cases, is still, on average, too small to guarantee a significant number of atmospheric re-entry for the disposed satellites (e.g., only about the the 4.6 % of all the disposed Galileo satellites in the investigated time frame).
Figures 5-6 show the perigee altitude distribution of the disposed satellites of the four constellations in the three simulation scenarios in year 2209.
Note the differences between the peaks in Figure 5, mainly related to the difference in traffic (hence number of satellites) between the constellations. The minimal interaction between the disposed GNSS spacecraft and the LEO protected region is noticeable. Checking also the apogee distribution, it can be noticed how, even in the Unstable case, where the maximal eccentricity growth is sought for, the interaction with the GEO protected zone is *de-facto* negligible.

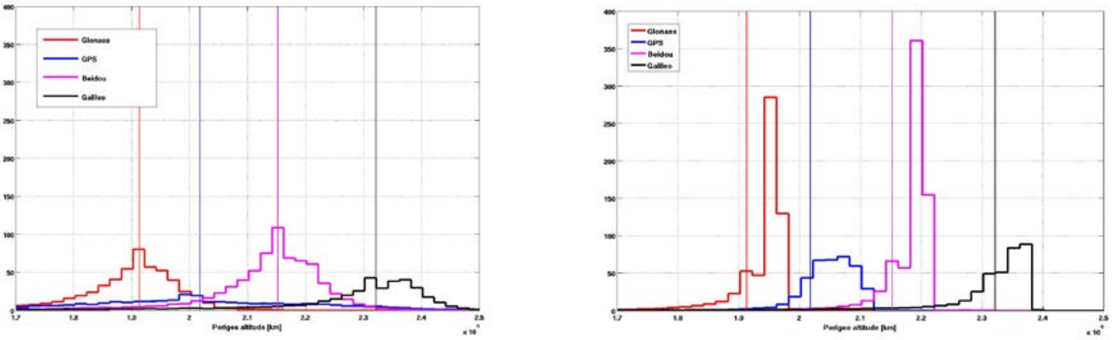

Figure 5. Perigee altitude distribution, in the year 2209, of the disposed satellites in the Reference (left) and Stable (right) scenarios. The thin vertical lines mark the altitude of the four GNSSs operational orbits.

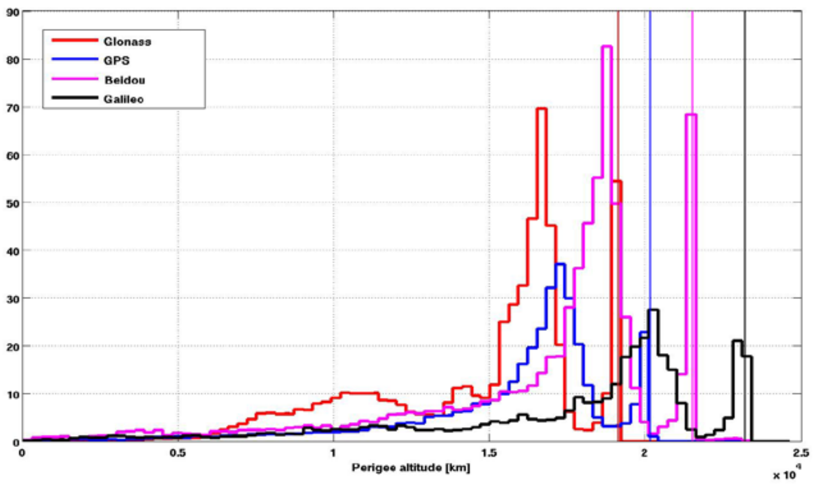

Figure 6. Perigee altitude distribution, in the year 2209, of the disposed satellites in the Unstable scenario. The thin vertical lines mark the altitude of the four GNSSs operational orbits.

6.2.1.2 Collision probability evolution

The situation described in the previous sections translates into a picture of the collision probability depicted by Figure 7. In the plot the overall collision expectancy for all the satellites (operational and disposed) of the four constellations is computed by cumulating over time all the collision probabilities stemming from orbital crossings, involving at least one GNSS object, as recorded by the CUBE algorithm.

Keeping in mind the Figure 5-6, it can be seen that the concentration of objects in the disposal zones, obtained in the Stable scenarios, while possibly advantageous in terms of operations for the GNSSs, is actually slightly increasing the probability of collision between uncontrolled object, in the long run (as also testified by the higher number of collisions recorded in the SDM runs for the Stable scenario, as detailed in Table 9).

It is worth stressing that operational satellites will be able to perform collision avoidance manoeuver, therefore it is reasonable to assume that most (if not all) the collision risk between operational satellites and other large, trackable intact objects can be reduced to negligible levels (see later for further discussions on the expected rate of avoidance manoeuvers). The right panel of Figure 7 shows the cumulated collision expectancy computed considering only cases where an uncontrolled satellite, from one of the GNSSs, is involved against any other uncontrolled object, i.e., other uncontrolled GNSS satellites, upper stages, MRO, fragments. In particular, in the specific figure, at least an uncontrolled satellites launched after the beginning of the simulation has to be

involved, in order to highlight the effects of the scenarios (i.e., a crossing between two uncontrolled GNSS satellites, both launched before the year 2009, is not included in the computation). Again it can be noted how the accumulation of uncontrolled objects in the disposal zones leads to higher values for the Stable scenario, with the Unstable slightly below the Reference one. This plot somehow summarizes the potential environmental effects of the simulated scenarios, since the potential collisions stemming from this collision expectancy cannot be avoided.
It is worth remembering that the actual value of the collision probability computed by CUBE depends from the geometry of an orbital crossing (i.e., trivially, the two objects must be in the same cube at the epoch of the time sampling) and from the velocity of the crossing. Since, as a matter of fact we are recording very few collisional fragmentations and a limited number of crossings in our simulations, a few *deep encounters* can actually unbalance the statistical computation of the cumulated collision expectancy.
Studying the actual number of crossings, in all the 50 MC runs, involving MEO objects for the three main scenarios some preliminary conclusions can be drawn. The largest number of crossings clearly involve disposed spacecraft. The most affected constellations are Glonass and Beidou and this is strictly related to their launch and traffic characteristics. The largest number of crossings, involving mainly disposed Glonass and Beidou spacecraft, is recorded in the Reference scenario. On the other hand the spreading of the disposal orbits in the Unstable scenario significantly decreases the total number of crossings, according to the so-called "dilution of collision risk". In particular, the crossing between *new objects* is strongly reduced whereas the number of crossings with *historical objects* is increased since the disposed objects in eccentric orbits tend to interact with other populations of objects in the MEO and upper LEO regions.
As was stated above, no feedback collisions are happening in all the MC runs. On the other hand, as seen in Figure 4 some collisional fragmentations are happening and therefore there are fragments spread around the MEO region. In all the scenarios the new fragments play a minor role, with about 100 crossings in all the 50 MC runs, i.e., about 2 crossings per MC run. The cumulative collision expectancy for all the GNSSs objects against fragments generated in the 200-year investigated time span (i.e., excluding fragments already present in space before the beginning of the simulations) remains below 10^{-2}, even after 200 years.
The plots in Figure 9 show the breakdown of the collision expectancy for the operational satellites within each constellation, coming from any other object. Whereas the collision risk for the operational satellites can be prevented, if a space surveillance system is in place, these plots can give an initial idea of the relative need for avoidance manoeuvers within the single GNSSs in the different scenarios.
Looking at the Figure 9 it can be noted how Galileo is facing systematically the lowest risk, due to its detachment in altitude from the other constellations. On the other hand, Glonass is always on top of the others, also due to larger number of objects (past and future) present in its altitude range.
Thanks to the higher statistics, the Glonass results in the three scenarios appear more separated showing how the so-called dilution of the collision probability, caused by the increased eccentricities of the disposed satellites, is indeed minimizing the cumulative collision expectancy for the Unstable scenario, which is about 30 % lower with respect to the other two. Then, the Reference and the Stable scenario show very similar cumulative collision expectancies. Note, however, that the number of orbital crossings follow a different pattern: summed over all the 50 MC runs, in the Reference scenario there are 289 crossings, in the Stable scenario there are 244 crossings and in the Unstable scenario there are 306 crossings. This means that, on average, the fewer encounters recorded in the stable case are indeed much deeper (lower relative velocity) than in the other scenarios and their weight in the low numbers statistics we are dealing with is more important.
It is important to note that, in the Stable case, the 34 % of the orbital crossing involving operational Glonass satellites are against disposed Glonass satellites. Nevertheless, at a closer look, it can also

be noticed how the majority of the disposed satellites involved in these crossings are actually *failed satellites*, i.e., satellites for which the disposal maneuver did not take place and that are left stranded at the operational altitude.

Whereas the encounters in the Unstable scenarios, due to the higher eccentricities, happens with geometric conditions leading to smaller values of the collision probability.

A similar behaviour is found in the other three constellations, with the results for the three scenarios less separated due to the lower statistics. For the GPS and the Galileo constellations, the values are much lower than those obtained for Glonass and Beidou. In particular, for Galileo it remains at the negligible level of 10^{-4} for the first 100 years, barely reaching 10^{-3} only after 200 years. This is due to a significantly lower number of orbital crossings recorded for the operational Galileo and GPS. Looking in detail to the overall number of crossings recorded for the Galileo operational spacecraft, in the 50 MC runs, it can be stated that the reference and unstable scenarios are more prone to orbital crossings of uncontrolled objects with the operational satellites.

The cumulative collision expectancy for operational Galileo satellites against disposed satellites from the same constellations was computed. As expected, in the Unstable scenarios the interaction between operational and disposed spacecraft is increased. The number of crossings is as follows: 17 in the Reference scenario, 12 in the Stable one and 24 in the Unstable one. It is, again, important to stress that, e.g., in the Stable case, out of the 12 crossings, 11 involve *failed disposed satellites*. Only one of the crossings pertains to a disposed satellites for which the disposal manoeuver was actually performed. The number of crossings between operational spacecraft and upper stages is even lower and is basically equal in the three scenarios.

In essence, we are dealing with very low numbers both in terms of overall number of crossings and in terms of collisions expectancies (below 10^{-3} even after 200 years). This makes it difficult to clearly discriminate the three scenarios and to draw firm conclusions. Nonetheless it appears reasonable to state that the Stable scenario minimizes the interaction between operational Galileo satellites and disposed Galileo satellites. Moreover, the importance of the reliability of the disposal manoeuver is once again highlighted.

Conversely, Figure 10 shows the cumulative collision expectancy for non-operational Galileo satellites against all other GNSS operational satellites in the three scenarios. The situation looks similar since the higher eccentricity reached by the disposed satellites in the Unstable scenarios brings them to an increased interaction with the other constellations. In particular, note that, in the Stable scenario, all the orbital crossings contributing to the plot in Figure 10 happen with disposed Galileo satellites, a part from a single crossing with a disposed Beidou satellite. On the other hand, in the Unstable case, the interaction of the disposed Galileo with the other constellations become apparent with the following orbital crossings. Whereas, the situation is clearly different between the two scenarios and is a clear indication of the expected trend.

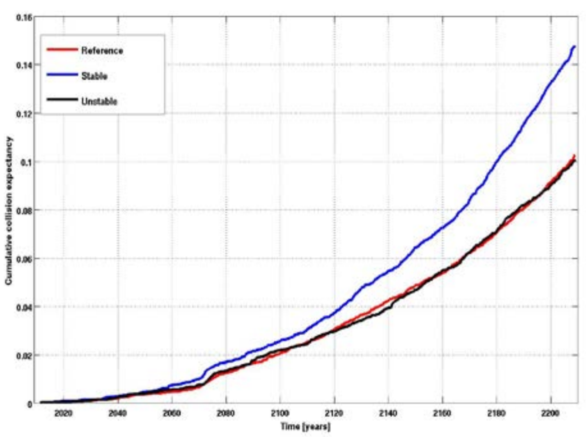

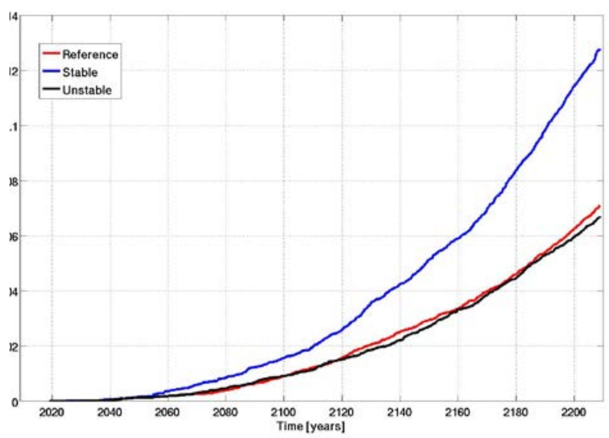

Figure 7. Left panel: cumulative collision expectancy for objects belonging to the GNSSs (both operational and disposed) in the three main scenarios: Reference (red), Stable (blue) and Unstable (black). Right panel: cumulative collision expectancy for non-operational objects belonging to the GNSSs against every other non-controlled object (i.e., other GNSSs non-operational, upper stages, fragments, MRO,....). See text for details.

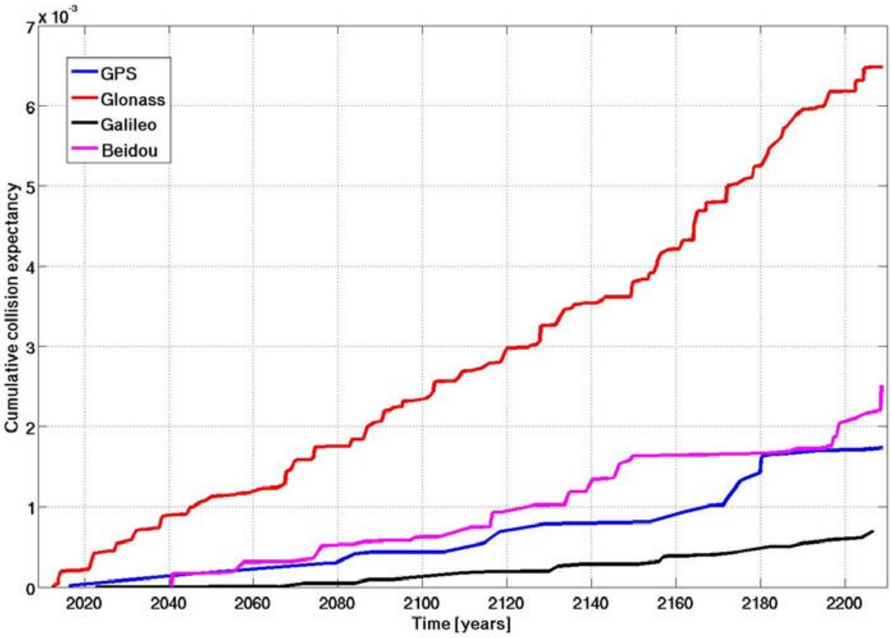

Figure 8. Cumulative collision expectancy for operational satellites belonging to the four GNSSs in the Reference scenario. The red line refers to Glonass, the blue line to GPS, the magenta line to Beidou and the black line to Galileo.

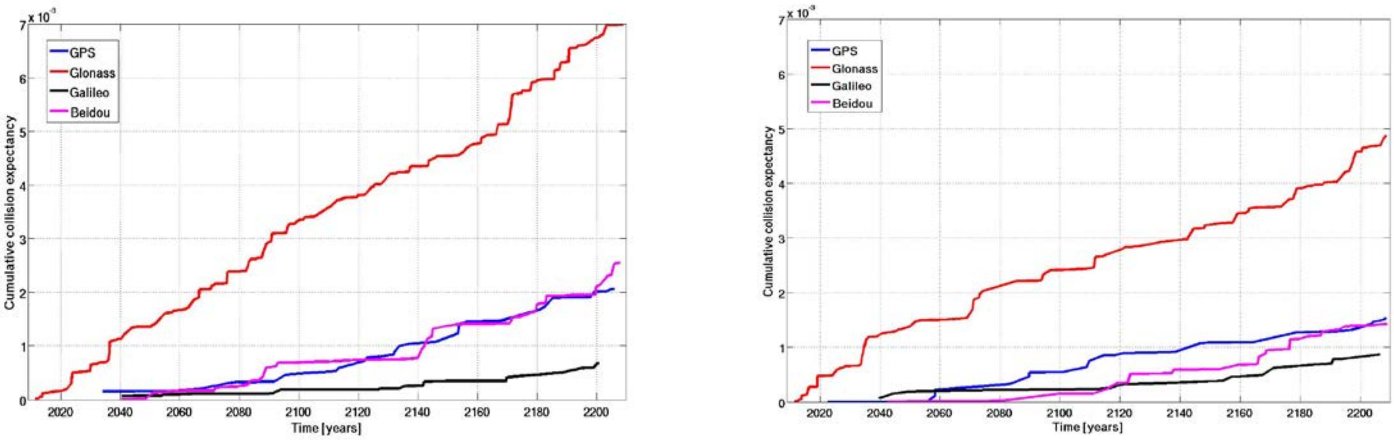

Figure 9. Cumulative collision expectancy for operational satellites belonging to the four GNSSs in the Stable (left panel) and Unstable (right panel) scenarios. The red line refers to Glonass, the blue line to GPS, the magenta line to Beidou and the black line to Galileo.

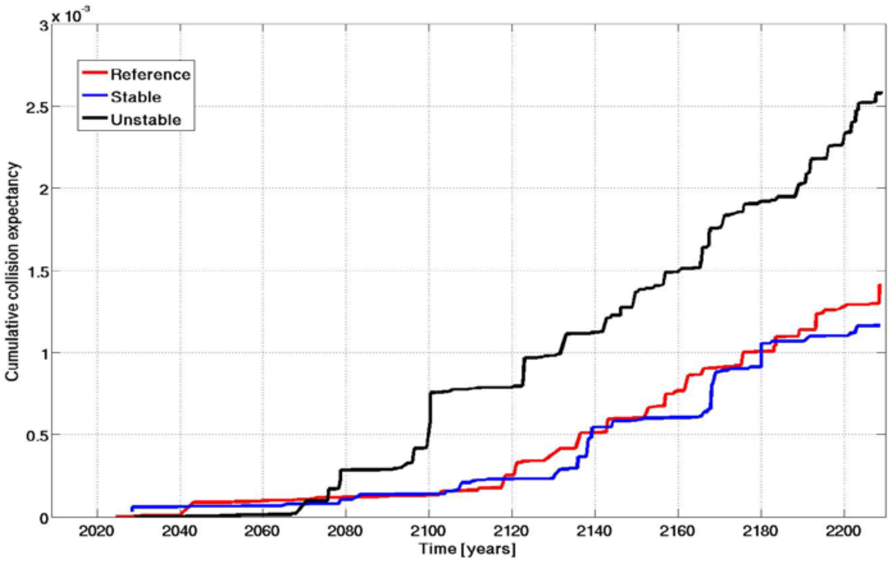

Figure 10. Comparison of the cumulative collision expectancy for non-operational Galileo satellites against all other GNSS satellites in the three scenarios: Reference (red), Stable (blue) and Unstable (black). See text for details.

6.2.2. Results of the scenario with inclination change

The Stable and Unstable scenarios were simulated again choosing, for every disposal, the matrix computed for the inclination closest to one of the spacecraft at the disposal epoch. These two new scenarios are dubbed Stable Inc. and Unstable Inc.

As a matter of fact, the results of these new scenarios are very similar to those described in Sec. 6.2.1.

The statistical measures of the eccentricity, at the end of the 200-year time span, for all the disposed GNSS satellites, in the two new scenarios are almost identical to those listed in Sec.6.2.1 for the standard scenarios, telling us that the effect of the slight inclination difference in the choice of the disposal orbits is not significant. Slightly higher values for the Unstable inclined scenario are found and this might be an indication of a possible improvement attainable with an optimized disposal strategy, taking into account the actual inclination of the satellites at the end-of-life. On the other hand, it is clear that, on average, over all the cases treated in the long term simulation described in this note, these small differences cannot play any significant role in the global picture.

In fact, comparing the cumulative collision expectancy in the new scenarios, with respect to three main cases shown in Figure 8, it can be clearly noticed how the new scenarios give substantially the same results, in terms of collision risks for the GNSSs. The only noticeable difference, with respect to the trend already seen in Figure 8, is that the Unstable case leads to a slightly reduced cumulative collision expectancy, which is not altering the general conclusions drawn in Sec.6.2.1.

As a general comments, it can be stated that the overall long-term statistical behaviour of the MEO environment in not significantly affected by possible inclination inaccuracies.

6.2.3. Results of the scenarios with Galileo only targeted disposal

The results of Sec. 6.3.1 confirm the conclusions already reached in previous works [12][13] calling for a global management of all the GNSSs, where the mitigation measures are harmonized between all the constellations. On the other hand, political, economical and practical reasons will most probably prevent the realization of this idealized scenario. Therefore we devised two new simulation scenarios where only the Galileo spacecraft are disposed targeting stable or unstable orbits. The other three constellations were instead managed following the Reference scenario. These two new scenarios were dubbed Stable Galileo and Unstable Galileo.

For the disposal of the Galileo spacecraft the method described in Sec. 6.2.2 (i.e., considering the actual inclinations of the spacecraft at end-of-life) was adopted. Therefore the two new scenarios have to be compared with the Reference scenario, the Stable Inc. and Unstable Inc. ones. Note that, at variance from the Unstable Inc. scenario, in the Unstable Galileo one *only the Galileo spacecraft are moved to an elliptic unstable orbit*.

The purpose of the two "Galileo only" scenarios is to check whether the application of targeted disposal policies, only for the Galileo constellations, are still useful for minimizing the collision risk and the avoidance manoeuver rate on the constellation itself.

Figure 81 and 82 show the cumulative collision expectancy for operational Galileo satellites against every other object, in the Stable Inc. and Unstable Inc. scenarios respectively (blue lines), compared with the similar cases of the Galileo-only cases (red lines). In both figures the Reference case is also shown (green lines) for comparison.

Comparing the cumulative collision expectancy for operational Galileo satellites as expected, only small differences can be noticed between the three main scenarios of Sec. 6.2.1 and the *Galileo-only* scenarios. Looking at the results of the Stable-Galileo case, it can be noticed how the Stable-Galileo is very similar to the Reference case and shows an increased collision expectancy with respect to the Stable Inclined case due, to the fact that the disposed spacecraft of the other constellations are actually placed in non-targeted orbits with possibly growing eccentricities.

In any case, it can be concluded that the detached orbit of the Galileo satellites makes them only marginally sensible to the management policies of the other three GNSSs.

On the other hand, a comment on the interaction between the disposed Galileo satellites and the other constellations, in this scenarios where only Galileo is performing disposal manoeuver. Of course, the results are similar to those shown in Figure 11 and the conclusions is that a minimal interaction is recorded for the Stable Galileo scenario, whereas an increased interaction is seen in the Unstable Galileo scenario. It must be stressed that the level of this interaction is very limited and thus it does not appear as a strong argument to prevent the adoption of a "dilution of collision risk" strategy.

6.3. Long term simulations: conclusions

The main results of the simulation campaign can be summarized as follows:

- In terms of the long term environment evolution, the Unstable scenario seems favourite. That is, if the focus is on the long term sustainability of the space environment, the possibility to dilute the collision risk and to aim at the re-entry in the atmosphere of a subset of the disposed GNSS spacecraft is the most attractive.
- The most "problematic" constellations are Glonass and Beidou. This conclusion is driven by the future launch traffic hypothesized for these constellations and by the past practices that left already a significant number of large uncontrolled spacecraft in the constellation orbital zone, in the case of Glonass.
- The Stable scenarios seems to minimize the interactions (crossings) with the operational constellations and, therefore, might be preferred for operational reasons. In particular, in the Stable scenarios the inter-constellations interaction is negligible.

- The Galileo constellation is well detached from the others and faces the lowest collision risks. This relates both to the interaction of the operational Galileo satellites with the disposed satellites from the other GNSSs and to the interaction between disposed Galileo satellites and the satellites belonging to the other GNSSs.
- Particular care should be devoted to the efficiency and reliability of the disposal manoeuvers. A significant share of the collision risk faced by the operational satellites in every simulated scenario can be traced back to the “failed” satellites (the success rate of the disposal manoeuvers was assumed to be 90 % for all the constellations).

7. Collision risk and expected manoeuver rate

Following the approach described in [6], a detailed analysis the collision risk against selected targets was performed. The output of the SDM simulations described in Sec. 6 is used as the background environment and a specific method detailed in the following section is used to identify the most relevant features of the collision risk over short periods of time. The possible need of avoidance manoeuvres is the different simulated scenarios is investigated too.

7.1. Comparing and calibrating the CUBE and Foster approaches

In parallel to the simulations described in the following sections, a DAMAGE study was performed to understand the consistency between the results generated using the CUBE/kernel and Foster-like algorithms implemented in DAMAGE, and to check the consistency between the collision probabilities estimated using DAMAGE and SDM.

The study outcome was that, as expected, the implementation of the Foster-like algorithm in DAMAGE depends heavily on the time-step that is used for the projection: longer time-steps lead to significant under-estimation of the collision rates unless a calibration/correction is used. For a time-step of 100 minutes, the calibration coefficient computed for the GNSS satellites was greater than 10^{7}. Given the magnitude of this correction, use of the Foster-like approach in the manner that is currently implemented is not recommended if relatively long time-steps are used: collision probability estimates are likely to be significantly in error. In contrast, at shorter time-steps the Foster-like method generates collision rates that are in-line with those produced by the CUBE/Kernel approach. Given that the CUBE/Kernel method also provides consistent collision rate estimates regardless of the time-step used, this method was determined to be the best choice for simulations over long time-periods and at default time-steps of the order of days.

The CUBE/Kernel method generated collision rates for the active and inactive GNSS satellite in orbit between $10^{-3.2}$ and $10^{-3.9}$ per year, depending on the epoch (higher rates at later epochs). These collision rates equate to a maximum accumulated collision probability of around 10^{-1} for all GNSS satellites, or values of the order 10^{-2} per constellation or 10^{-3} per satellite over a 200-year period. These results are in good agreement with the results found using the SDM code (see, e.g., Figure 9) and, therefore, provide some confidence in the results reported using that model.

7.2. The post-processing setup

The simulation setup is as follows:

- The overall debris environment obtained as output of the SDM simulations described in [3] is used as the “background” population against which a selected “target” object is flown. That is, in a post-processing phase the orbit of a target object is propagated, along with the orbits of all the background population and the orbital crossings are recorded.
- Each object has its own (diagonal) covariance matrix according to the orbital regime (LEO-MEO-GEO).
- The CUBE algorithm [7] is used as a filter to identify orbital crossings. For this purpose, CUBE is evaluated with a much shorter time-step of 10^{-4} days (i.e., 8.64 sec). The time step

is chosen to be short enough to catch most of the orbital crossings, while keeping the computational burden to an acceptable level. It is worth remembering that the standard CUBE evaluation time step for an SDM run is 5 days.

- To cumulate statistics, at each evaluation time step, the anomalies of the population objects (projectiles) are randomized and the CUBE evaluation is performed for the 500 randomized anomalies (resulting in a local Monte Carlo experiment).
- Every time, in anyone of the 500 MC occurrences, two objects are found within an enlarged cube ($30 \times 30 \times 30$ km^3) the collision probability is evaluated with the Foster algorithm [6].
- Due to the heavy computational burden, related to the short time steps and the large number of MC evaluations, 1-month snapshots are evaluated at different epochs (e.g. in the years 2009, 2029, 2059, 2109, etc.).

7.3. The simulations

A number of test targets were considered in different orbital regimes. Of course particular care was devoted in evaluating the collision risk within the GNSSs, by considering the interaction between disposed satellites from all the fours constellations against every other object belonging to the constellations themselves. Moreover, the interaction between disposed GNSS satellites and other orbital zones, such as LEO and GEO, was investigated.
Note that, since we are interested in the possible interactions between the disposed GNSS objects and the selected target objects, only the orbital crossings involving GNSS related objects are analysed. All the other crossings are neglected in the analysis that follows.

7.4. LEO and GEO interactions

To test the possible interaction between disposed GNSSs satellites and the LEO and GEO protected zones, the orbital intersections against selected objects in those regions were computed.
In particular, for LEO, the selected targets are listed in the following Table:

	Semiaxis [km]	Eccentricity	Inclination [deg]	Area of spacecraft [m^2]
Envisat	7073	0.0013	98.4	40
ISS	6790	10^{-5}	51.65	100
Spacecraft at 1400 km	7803	0.002	82.07	9.297

For the Envisat case both a Reference scenario and the Unstable scenario were simulated, that is the post-processing was run using the background population produced in both the scenarios. The epochs considered for the 1-month snapshots were the years 2009, 2159 and 2209.
The results for the LEO orbits were *de-facto* null. Not a single orbital crossing between the target orbits and the disposed GNSSs satellites was recorded for the ISS and Envisat cases. In the case of the spacecraft at 1400, 11 crossings with disposed Beidou satellites were recorded by the CUBE pre-filtering in the year 2209 case, but all of them had collision risk below 10^{-50}. According to the Foster algorithm, the closest approach in the 11 cases happened at a distance of about 15 km.
This is clearly related to two main facts:

- as seen in Sec 6.3, a limited number of disposed GNSS satellites actually reach the LEO protected zone within the 200-year investigated time span;
- even for the small number of disposed MEO objects actually crossing LEO, this happens only at the perigee of highly elliptical orbits. This means that these object spend most of their time at apogee well above LEO. Therefore the cumulated time in LEO is so small that there is indeed a negligible interaction with the LEO population.

Similarly for the GEO protected region the test target objects were:

	Semiaxis [km]	Eccentricity	Inclination [deg]	Area of spacecraft [m^2]
Meteosat	42165	0.00001	0.11	12
Artemis	42165	0.0002333	11.8	125

Moreover a target in an inclined geosynchronous orbit, namely a satellite of the GEO component of the Beidou system, was considered:

	Semiaxis [km]	Eccentricity	Inclination [deg]	Area of spacecraft [m^2]
Beidou-GEO	42163	0.003	55.0	25

For the Meteosat case, both a Reference scenario and an Unstable scenario were simulated, while for the other two cases only the Unstable scenario was considered.
In the GEO low inclination cases (1 and 2) a crossing (in all the 500 MC runs considered) was recorded between Meteosat and a disposed Galileo satellite in the year 2209 and a crossing between Artemis and a disposed Beidou in the year 2209, both in the Unstable scenarios. Both encounters had collision risks below 10^{-50}, with the closest approach at more than 60 km.
The negligible interaction can be traced back to the fact that the crossing can happen around the apogee of the elliptical inclined orbit of the disposed GNSS objects and the target circular GEO orbit. An orbital crossing is possible only when the line of apsides of the orbit of the disposed object is at a given phase in its rotation within the orbital plane. Therefore only a limited number of configurations, for a short fraction of the lifetime of the disposed object, are leading to actual crossings in the 3D space, even if the apogee altitude is at the level of the GEO protected zone. This geometrical aspect, together with limited number of disposed GNSSs satellites reaching GEO at apogee, accounts for the negligible interaction.
A different geometry and, hence, a different collision risk if faced by the Beidou satellites in the geosynchronous inclined orbit.
In this case a limited interaction with GNSS satellites is found, for a total of 10 orbital crossings with disposed Galileo satellites and of 1 orbital crossings with disposed Beidou-M satellites, in the 500 MC, in the year 2209. None of these orbital crossings had a collision risk above zero and the closest approach recorded was at about 14 km. No interaction was found for the epoch of 2159.
Note that, in the Beidou-GEO case (and partly in the Meteosat case), a significantly larger number of orbital crossings are recorded against upper stages in GTO orbits.
It can therefore be concluded that, irrespective of the strategy adopted, the interactions between the disposed GNSSs spacecraft and the LEO and GEO protected zones is *de-facto* negligible, both in absolute terms (i.e., considering the actual orbital crossings) and, even more, in relative terms, taking into account the background collision risk in those regions, due to the resident objects.

7.5. HEO interactions

The interaction with objects in highly elliptical orbits, periodically crossing MEO, was tested too. The targets considered were:

	Semiaxis [km]	Eccentricity	Inclination [deg]	Area of spacecraft [m^2]
Proba 3	36943	0.8111	59.0	3
Ariane 5 U/S	24445	0.7167	5.0	28

The simulations were performed, for both cases, considering the three scenarios Reference, Stable and Unstable, in the epochs 2059, 2109, 2159 and 2209.

For the Proba 3 spacecraft the maximum number of orbital crossings was recorded in the Unstable case at the 2209 epoch. The main interaction is with disposed Beidou and disposed Glonass satellites (38 and 31 orbital crossings respectively). Four encounters with disposed GPS satellites and no orbital crossings with Galileo spacecraft were recorded. Note that these results can be considered mostly a product of the different population sizes, i.e. of the larger number of uncontrolled Beidou and Glonass satellites left in space, and not particularly related to the orbital characteristics of these abandoned spacecraft. All the crossings gave negligible values of the collision risk (always below 10^{-30}), even though in a few cases the closest approach distance was of the order of 5 km.
The other sample target in highly elliptical orbit considered was an Ariane 5 upper stage in Geostationary Transfer Orbit. There is an increased interaction of the GTO with the GNSS related objects proven by the higher number of orbital crossings, with respect to the one obtained for the Proba 3 case In particular, for the Ariane 5 target, all the four constellations are involved. E.g., in the Unstable scenario, at the 2209 epoch, 69 Beidou, 49 Glonass, 40 GPS and 48 Galileo crossings are detected by the CUBE pre-filtering. Nonetheless, also in this case all the crossings have very low values of the collision probabilities, with the no significant differences between the two simulated scenarios. Again, the highest values of the computed collision risk (still below 10^{-30}) is found in a few orbital crossings with closest approach distances of the order of 4 – 5 km.
In terms of the level of the interaction for the four constellations, we note that Beidou experiences the highest number of orbital crossings, followed by Glonass and Galileo, with a similar number of occurrences, while GPS is much less involved. It is also worth stressing that a very limited number of crossings is recorded between the Ariane 5 target and operational satellites of Glonass, GPS and Galileo.

7.6. GNSS interaction

The collision risk faced by the operational constellation satellites against all the other GNSS related objects was checked. For each constellation, a satellite on the operational orbit was selected as the test target. The following plots show the interaction only against objects related to the GNSSs, to highlight the effects of the different simulated scenarios. The interaction against the background objects transiting in MEO is considered similar for all the tested target and is therefore not shown and discussed.
The test performed are listed in Table 12.

	Semiaxis [km]	Eccentricity	Inclination [deg]	Area of spacecraft [m^2]
Operational Glonass sat.	26560	0.005	55	20
Operational GPS satellite	25508	0.001	65	16.7
Operational Beidou sat.	27906	0.001	55	20
Operational Galileo sat.	29600	0.0005	56	11

Table 12: Orbital and physical characteristics of the simulated GNSS target objects.

For all the above cases the three main scenarios (Reference, Stable and Unstable), described in [3], were simulated, in one-month snapshots at 5 different epochs: 2009, 2059, 2109, 2159 and 2209.
Furthermore, for the Galileo constellation, the existence of possible asymmetries in the collision risk on the constellation planes was tested by computing the collision risk on an operational satellite located on a different constellation plane (i.e., having the same semimajor axis, eccentricity and inclination, but a different RAAN, separated by 120 degrees).

In all the following analysis it was decided to set a limit to the lowest recorded value for the collision probability computed during a close encounter. This limit was set somehow arbitrarily to 10^{-50}. All the probability values below this threshold are considered to be zero.

7.6.1. GPS

From a global point of view, the first comment is that considering all the epochs and all the scenarios simulated for the GPS target orbit, only 6 crossings resulted in a probability above the threshold. The highest value computed equals 2.5 x 10^{-9}, in an orbital crossing against an abandoned upper stage.
The following Table details the result for each scenario. In the first three columns there are the numbers of crossings that result in a collision risk higher than the above mentioned threshold of 10^{-50}. In the fourth column there is the highest computed value for the collision risk for each scenario. The columns from 5 to 8 give the number of crossings with distance lower than 100 km, then, from 9 to 11 the crossing with distance below 10 km and from 12 to 15 the crossings with distance below 2 km. Finally, the last column gives the minimum computed distance in all the crossings for a given scenario.

	Number of crossings with P>10^{-50}			**Max value of P**	**Number of crossings with D<100 km**			**Number of crossings with D<10 km**			**Number of crossings with D<2 km**			**Min. value of D [km]**
	2009	**2109**	**2209**		**2009**	**2109**	**2209**	**2009**	**2109**	**2209**	**2009**	**2109**	**2209**	
REF	1	1	0	1.7×10^{-22}	429	1306	1494	3	16	29	1	2	1	1.360
STAB		0	1	2.5×10^{-9}		1072	1398		10	37		1	2	0.277
UNST		0	0	0		1205	2596		8	53		1	0	1.81

Table 13: Details of the orbital crossings for the GPS target orbit (see text for details).

As mentioned above, none of the orbital crossings has a probability high enough to trigger a collision avoidance manoeuvre. On the other hand, the orbitals crossing with distance below 10 km can be close enough to, at least, require additional tracking and scrutiny by the ground control (nonetheless it is worth stressing that the numbers in the table refer to the total recorded in the 500 MC random draw of the mean anomaly of the "projectile" population, hence we are looking at about 1/10 of crossing below 10 km per scenario, in the investigated month in the year 2209). In this case it can be noticed how the Unstable case shows the highest number of occurrences, even though the Reference and Stable scenario are quite close.
Concerning the objects crossed, in the Stable case, the vast majority of the crossings are against disposed GPS satellites (actually, mostly against failed satellites that were not really removed from the operational orbit), with a limited number of crossings against disposed Glonass, thanks to the limited eccentricity growth of the abandoned satellites. In the Reference scenario there is an increased interaction with the uncontrolled disposed Glonass satellites. On the other hand, in the Unstable scenario, beyond a larger interaction with disposed GPS satellite, a significant number of crossings against disposed Glonass and, also, Beidou satellites is found. A small number of crossings against disposed Galileo satellites is noticeable too. The collision risk related to disposed satellites is significantly higher than the one against upper stages, partly due to the different number of these objects present in the considered region of space.

7.6.2. Glonass

The results of the Glonass scenarios point to the same conclusions as in the GPS cases.
Considering all the epochs and all the scenarios simulated for the GPS target orbit, only 15 crossings resulted in a probability above the threshold. The highest value computed equals 1.12 x 10^{-6}.

Considering the orbital crossings, it can be noticed how the collision risk related to disposed satellites is significantly higher than the one against upper stages, partly due to the different number of these objects present in the considered region of space. In the Stable case, the vast majority of the crossings are against disposed Glonass satellites, both historical and new, i.e., launched after the beginning of the simulation (actually, mostly against failed satellites that were not really removed from the operational orbit). A moderate interaction is also found with disposed GPS satellites. In the Unstable scenario, beyond a larger interaction with disposed Glonass satellite, a significant number of crossings are recorded against disposed GPS and Beidou satellites.
As in the GPS cases, the increased interaction in the Unstable case is noticeable from Table 13. Again, even though the highest value of the collision risk computed is not enough to trigger an avoidance manoeuvre, more than 100 crossings with distances below 10 km are recorded in the 500 MC occurrences.

	Number of crossings with $P>10^{-50}$			Max value of P	Number of crossings with D<100 km			Number of crossings with D<10 km			Number of crossings with D<2 km			Min. value of D [km]
	2009	2109	2209		2009	2109	2209	2009	2109	2209	2009	2109	2209	
REF	1	1	1	$1.32x10^{-7}$	2959	3390	3313	136	59	74	3	1	1	0.81
STAB		3	0	$1.12x10^{-6}$		3857	4468		96	92		5	4	0.756
UNST		0	6	$2.76x10^{-25}$		6688	6855		104	136		1	3	1.12

Table 14: Details of the orbital crossings for the Glonass target orbit (see text for details).

7.6.3. Beidou-M

Similar considerations can be drawn, as in the GPS and Glonass cases, for the Beidou-M target orbit. Considering all the epochs and all the scenarios simulated for the Beidou-M target orbit, only 7 crossings resulted in a probability above the threshold. The highest value computed equals 1.03×10^{-6}.

	Number of crossings with $P>10^{-50}$			Max value of P	Number of crossings with D<100 km			Number of crossings with D<10 km			Number of crossings with D<2 km			Min. value of D [km]
	2009	2109	2209		2009	2109	2209	2009	2109	2209	2009	2109	2209	
REF	1	0	0	$2.8x10^{-28}$	377	2351	1837	3	51	28	0	1	1	1.360
STAB		0	1	$7.7x10^{-30}$		1849	1926		83	37		2	1	0.969
UNST		0	3	$1.03x10^{-6}$		1785	2721		52	72		0	2	0.91

Table 15: Details of the orbital crossings for the Beidou-M target orbit (see text for details).

7.6.4. Galileo

Considering all the epochs and all the scenarios simulated for the Galileo target orbit, only 10 crossings resulted in a probability above the threshold. The highest value computed equals 2.26×10^{-8}.
Looking at the number of crossing within 100 km, in Table 16, the increased interaction in the Reference and Unstable case is noticeable, even though the three scenarios are quite close. Also the number of closer crossings is indeed comparable and very low (less than 1/10 of close passage for every MC occurrence in one month of the 2209 cases).
As mentioned above, the majority of the collision risk is coming from uncontrolled satellites that failed to perform the disposal manoeuvre and were left stranded in the operational orbit.

	Number of crossings with $P>10^{-50}$			Max value of P	Number of crossings with D<100 km			Number of crossings with D<10 km			Number of crossings with D<2 km			Min. value of D [km]
	2009	2109	2209		2009	2109	2209	2009	2109	2209	2009	2109	2209	
REF	1	0	0	2.26×10^{-8}	128	808	1513	1	24	27	1	0	1	1.360
STAB		1	0	6.4×10^{-45}		789	1497		28	38		0	3	1.262
UNST		1	1	1.51×10^{-18}		1312	1589		28	36		1	1	1.05

Table 16: Details of the orbital crossings for the Galileo target orbit (see text for details).

7.6.5. Galileo planes

To highlight possible asymmetries in the distribution of the collision risk, the results obtained for the operational Galileo satellite listed in Table 1 were compared with those obtained for a satellite with the same characteristics, but with a RAAN incremented by 120 degrees, i.e., belonging to a different constellation plane. A single epoch (the year 2159) was investigated.

	Number of crossings with $P>10^{-50}$		Max value of P		Number of crossings with D<100 km		Number of crossings with D<10 km		Number of crossings with D<2 km		Min. value of D [km]	
	P 1	P 2	P 1	P 2	P 1	P 2	P 1	P 2	P 1	P 2	P 1	P 2
REF	2	3	2.26×10^{-8}	1.61×10^{-18}	1122	1071	36	37	2	3	0.74	0.68
STAB	0	0	0	0	1231	1113	31	18	0	0		
UNST	0	2	0	4.62×10^{-14}	1371	1534	32	39	1	2	1.74	0.89

Table 17: Details of the orbital crossings for the two considered planes of the Galileo constellation (see text for details). P1 refers to the plane number 1 and P2 to the plane displaced by 120 degrees from it.

Table 26 displays very similar number for the two different planes. This is expected since there is no obvious mechanisms to generate asymmetries in the distribution of the collision risk in the considered scenarios. Some differences are well explained by, e.g., the randomness in the selection of the planes where a given satellite fails, or particular mutual orientations of the constellations planes at the epochs considered.
Therefore, it can be concluded that no particular influence of the different constellation planes on the overall collision risk is found.

7.7. Collision risk conclusions

Looking in detail to short time spans the main features, advantages and disadvantages, of the scenarios simulated in [3] can still be noticed.
As expected, due to orbital characteristics, the interaction of the disposed GNSS satellites with the LEO and GEO protected zones is negligible, both in absolute terms and, even more, compared to the background risk in those regions of space.
For the operational GNSS spacecraft, the highest interaction with other MEO objects is generally recorded in the Unstable scenarios. In none of the scenarios considered a collision risk higher than the thresholds commonly adopted for collision avoidance was ever recorded, Only a few crossings with probability higher than 10^{-6} were found. This is related to the very low spatial density of objects in the MEO region, which makes orbital crossings statistically rare events.

The low interaction of the Galileo constellation with the other three GNSS is confirmed. The majority of the risk for operational Galileo comes from disposed Galileo spacecraft and from GNSS related upper stages.
In all the constellations, and in particular for Galileo, the role of the "failed" satellites appears of paramount importance. Most of the intra-constellation collision risk is due to satellites that were not able to manoeuvre out of the operational zone, thus somehow nullifying the efforts made in devising optimal complex mitigation strategies.
The analysis of the collision risk on two different Galileo constellation planes (with RAAN separated by 120 degrees) did not show the evidence of any effect related to the considered plane. That is, there is no notable angular asymmetry in the distribution of the collision risk for the Galileo planes.

8. Conclusions

The main results of the Contract are summarized in the following bullets.

Concerning the theoretical analysis of the MEO phase space:

- The numerical investigation of the MEO phase space allowed us to identify the values for the argument of perigee ω corresponding to any given combination of initial epoch, longitude of ascending node and inclination (t_0, Ω, *i*), which ensure in 200 years stability or instability of the orbital evolution of a disposed satellite in MEO. At the moment there does not exist an analytical formulation to find these initial conditions, but the work carried out has given a very significant boost in this direction, deriving both from the results computed numerically and the analytical treatment we have developed in terms of overlapping resonances, which are responsible of the chaotic behaviour detected.
  It turns out that we are almost always able to provide initial conditions which can be considered safe over 200 years (except for GLONASS), but we cannot always define initial conditions which lead to an Earth re-entry. This is due to the fact that in practice we do not have the freedom to change (Ω, *i*) to get a more favourable positioning, but more importantly to the intrinsic dynamics where these satellites live. According to the Chirikov criterion, chaos occurs whenever two or more orbital resonances interact, and implies a non-predictability of the long-term behaviour of the bodies. The chaotic zones defined by the regions of overlapping resonances do not preclude the existence of regular trajectories embedded within it. Indeed, the character of the motion depends sensitively upon the initial orientation angles of the satellite and the initial lunar node. This is revealed by the fact that we found large stable regions in the graveyard case for each constellation, even though the constellations exist in such precarious states in the *e*-*i* phase space, always perched on the threshold of instability. The chaoticity of this region also has a further important implication: no matter how accurate our model, once a dynamical instability sets in, the subsequent evolution is unpredictable in detail.

The study of future possible means of active de-orbiting of the Galileo satellites lead us to the conclusions that:

- A 6 months deorbiting achievable with a low-thrust engine with T=0.2 or 0.3 N
- The best low-thrust strategy is the one that aims at increasing the eccentricity, however a different re-entry angle is achieved than re-entering with a spiralling trajectory.
- If the low-thrust engine has a limit of 0.1 N thrust for 6 month operational time, a deployable device can be also used afterwards with SRP modulation for completing the deorbiting phase.

The main results of the long term simulation campaign can be summarized as follows:

- In terms of the long term environment evolution, the Unstable scenario seems favourite. That is, if the focus is on the long term sustainability of the space environment, the possibility to dilute the collision risk and to aim at the re-entry in the atmosphere of a subset of the disposed GNSS spacecraft is the most attractive.
- The most "problematic" constellations are Glonass and Beidou. This conclusion is driven by the future launch traffic hypothesized for these constellations and by the past practices that left already a significant number of large uncontrolled spacecraft in the constellation orbital zone, in the case of Glonass.
- The Stable scenarios seems to minimize the interactions (crossings) with the operational constellations and, therefore, might be preferred for operational reasons. In particular, in the Stable scenarios the inter-constellations interaction is negligible.
- The Galileo constellation is well detached from the others and faces the lowest collision risks. This relates both to the interaction of the operational Galileo satellites with the disposed satellites from the other GNSSs and to the interaction between disposed Galileo satellites and the satellites belonging to the other GNSSs.
- Particular care should be devoted to the efficiency and reliability of the disposal manoeuvers. A significant share of the collision risk faced by the operational satellites in every simulated scenario can be traced back to the "failed" satellites (the success rate of the disposal manoeuvers was assumed to be 90 % for all the constellations).

Concerning the collision risk analysis the main conclusions are as follows:

- As expected, due to orbital characteristics, the interaction of the disposed GNSS satellites with the LEO and GEO protected zones is negligible, both in absolute terms and, even more, compared to the background risk in those regions of space.
- For the operational GNSS spacecraft, the highest interaction with other MEO objects is recorded in the Unstable scenarios.
- The low interaction of the Galileo constellation with the other three GNSS is clearly confirmed. The majority of the risk for operational Galileo comes from disposed Galileo spacecraft and from GNSS related upper stages.
- In all the constellations, and in particular for Galileo, the role of the "failed" satellites appears of paramount importance. Most of the intra-constellation collision risk is due to satellites that were not able to manoeuvre out of the operational zone, thus somehow nullifying the efforts made in devising optimal complex mitigation strategies.
- The analysis of the collision risk on two different Galileo constellation planes (with RAAN separated by 120 degrees) did not show the evidence of any effect related to the considered plane. That is, there is no notable angular asymmetry in the distribution of the collision risk for the Galileo planes.
- Finally, one of the expected outcomes of this study was the manoeuvre rate for each of the simulated scenarios. As a matter of fact, none of the orbital crossings actually triggered a manoeuvre, even considering a very low threshold of 10^{-5}. This is related to the very low spatial density of objects in the MEO region, which makes orbital crossings statistically rare events.

9. References

[1] Anonymous, *Semi-analytic Tool for End of Life Analysis software (STELA) User's Guide*, Version 1.4, Centre National d'Etudes Spatiales (CNES), Paris, France, July 2011.

[2] Bond, P.R., Endres, M. (Eds.), *HIS Jane's Space Systems & Industry (2012-2013)*, HIS Global Limited, Redhill, Surrey, UK, 2012.
[3] Chao, C.C., MEO Disposal Orbit Stability and Direct Reentry Strategy, in: *Spaceflight Mechanics 2000*, Advances in the Astronautical Sciences Series, Vol. 105, Part II, Univelt Inc., San Diego, California, pp. 817-838, 2000.
[4] Chao, C.C., Gick, R.A., Long-Term Evolution of Navigation Satellite Orbits: GPS/GLONASS/GALI-LEO, *Advances in Space Research*, 34, 1221–1226, 2004.
[5] Colombo, C., McInnes, C.R., Orbital Dynamics of 'Smart Dust' Devices with Solar Radiation Pressure and Drag, *Journal of Guidance, Control, and Dynamics*, 34, 1613-1631, 2011.
[6] Foster , J., The Analytic Basis for Debris Avoidance Operations for the International Space Station, *Proceeding of the Third European Conference on Space Debris*, ESA SP-473, pp. 441-445, 2001.
[7] Liou, J.-C., Collision Activities in the Future Orbital Debris Environment, Adv. Space Res., 38, 2102–2106, 2006.
[8] Lücking, C., Colombo, C., McInnes, C.R., Mission and system design of a 3U CubeSat for passive GTO to LEO Transfer, in: *Proceedings of the 63rd International Astronautical Congress*, Naples, Italy, Paper IAC-12-E2.1.4, 2012.
[9] Merz, K., *Reference Galileo Constellation*, e-mail of the ESA Study Manager to the Contractor, ESA Contract on Disposal Strategies Analysis for MEO Orbits, July 5, 2013.
[10] Merz, K., *Review of GNSS Orbital Data*, Memo MEO-DISP-001-KM, ESA/ESOC, July 10, 2013.
[11] Rossi, A., Resonant dynamics of Medium Earth Orbits: space debris issues, *Celest. Mech. Dyn. Astr.*, 100, 267-286, 2008.
[12] Rossi A., Valsecchi G.B. and Perozzi E., Risk of collision for the navigation constellations: the case of the forthcoming Galileo, *The Journal of the Astronautical Sciences*, 52, 455-474 (2004).

[13] Rossi A., Anselmo L., Pardini C. and Jehn R., Effectiveness of the deorbiting practices in the MEO region, *Proceedings of the 5th European Conference on Space Debris* (ESA SP-672). 30 March - 2 April 2009, ESA/ESOC, Darmstadt, Germany. Editor: D. Danesy (2009)